

1 Differences in MOPITT surface-level CO retrievals and trends from Level 2 and Level 2 3 products in coastal grid boxes

3

4 Ian Ashpole¹ and Aldona Wiacek^{1,2}

5

6 ¹Department of Environmental Science, Saint Mary's University, Halifax, Canada

7 ²Department of Astronomy and Physics, Saint Mary's University, Halifax, Canada

8 *Correspondence to:* Ian Ashpole (ian.ashpole@smu.ca)

9

10

11 **Abstract**

12

13 MOPITT retrievals are more sensitive to near-surface CO when performed over land than water. Data users
14 are therefore advised to discard retrievals performed over water from analyses to limit the a priori influence
15 on results. Level 3 (L3) products are a 1° x 1° gridded average of finer resolution Level 2 (L2) retrievals. For
16 coastal grid boxes, these are retrievals that are either performed over land, water, or a combination of the
17 two, on any given day. L3 data users therefore have limited ability to filter for retrievals performed over
18 water for these grid boxes. The consequences that this has on surface-level retrievals and their temporal trends
19 in “as-downloaded” L3 data (“L3O”) are examined in this paper, for all coastal L3 MOPITT grid boxes (n =
20 4299), by comparison to separate land- and water-only grid box averaged L2 retrievals (“L3L” and “L3W”,
21 respectively). First, it is established that mean retrieved VMRs in L3L and L3W differ by over 10 ppbv,
22 significant (p < 0.1) at 60 % of the coastal grid boxes. Trends are also stronger in L3L (mean difference
23 between 0.28 ppbv y⁻¹ and 0.43 ppbv y⁻¹), with the L3L – L3W trend difference significant at 36 % of grid
24 boxes. These L3L – L3W differences are clearly linked to retrieval sensitivity differences, with L3W being
25 more heavily tied to the a priori CO profiles used in the retrieval, which are a model-derived monthly mean
26 climatology that, by definition, has no trend year-to-year. On days when L3O is created from the averaging
27 together of L2 retrievals over both land and water (L3O_M), the result is VMRs that are significantly different
28 to L3L for 45 % of all coastal grid boxes, corresponding to 75 % of grid boxes where the L3L – L3W
29 difference is also significant. Just under half of the grid boxes that featured a significant L3L – L3W trend
30 difference also see trends differing significantly between L3L and L3O_M. Factors that determine whether
31 L3O_M and L3L differ significantly include proportion of the surface covered by land/water, and the
32 magnitude of sensitivity contrast. Comparing the full L3O dataset to L3L, it is shown that if L3O is filtered
33 so that only retrievals over land (L3O_L) are analysed, there is a huge loss of days with data. This is because
34 L2 retrievals over land are routinely discarded during the L3O creation process, for coastal grid boxes. The

35 problem can be lessened by also retaining L3O_M retrievals, but the resulting L3O “land or mixed” (L3O_{LM})
36 subset still has less data days than L3L for 61 % of coastal grid boxes. Moreover, these additional days with
37 data feature some influence from retrievals made over water that can affect results. Coastal L3 grid boxes
38 contain 33 of the 100 largest coastal cities in the world, by population. Focusing on the L3 grid boxes
39 containing these cities, we ask whether results of analyses are significantly different if using L3O compared
40 to L3L. It is shown that mean VMRs in L3O_L and L3L differ significantly for 11 of the 27 grid boxes that
41 can be compared (there are no L3O_L data for 6 of the grid boxes studied). The L3L – L3O_{LM} mean VMR
42 difference exceeds 10 (22) ppbv for 11 (3) of the 33 grid boxes, significant in 13 cases. 9 of the 18 grid boxes
43 where WLS analysis can be performed in L3O_L feature a trend that is significantly different to L3L. The
44 trends in L3O_{LM} and L3L differ significantly for 5 of the 33 grid boxes. It is concluded that a L3 product
45 based only on L2 retrievals over land – the L3L product analysed in this paper, available for public download
46 – could be of benefit to MOPITT data users, given the significant differences in mean CO VMRs and trends
47 that can be obtained for coastal grid boxes using L2 products in which retrievals performed over water can
48 be more easily discarded.

49
50

51 **1. Introduction**

52

53 Carbon monoxide (CO) is directly emitted into the atmosphere from anthropogenic (e.g. fossil fuel burning)
54 and natural (e.g. wildfire) sources, and also produced via the oxidation of hydrocarbons in the atmosphere.
55 With an atmospheric lifetime of weeks to months (e.g. Duncan et al., 2007), it is an important tracer of
56 pollutant transport and indicator of emission sources. While a health concern in its own right at high enough
57 concentrations, CO also plays an important role in atmospheric chemistry, for example as a precursor to
58 ozone formation and a primary sink for the hydroxyl radical. Atmospheric CO concentrations have decreased
59 since the start of the 21st century, with a slowdown in the rate of decline observed in recent years (Buchholz
60 et al., 2021). Trends also show substantial spatial variability (Hedelius et al., 2021). Satellite instruments
61 have been central to our understanding of global change in CO concentrations, with the Measurement of
62 Pollution in the Troposphere (MOPITT – Drummond et al., 2010, 2016) instrument well suited to this task,
63 providing a nearly-unbroken and consistent data record since the year 2000.

64 MOPITT observes upwelling radiances at thermal infrared (TIR) and near infrared (NIR) wavelengths
65 and uses these in an optimal estimation retrieval algorithm to retrieve coarse vertical resolution CO profiles,
66 which are integrated to give total column amounts. Among multiple additional inputs required by the retrieval
67 algorithm, a priori CO profiles – which describe the most probable state of the CO profile at a given location
68 – are necessary to constrain the retrieval to physically reasonable limits (Pan et al., 1998; Rodgers, 2000; the

69 retrieval algorithm is outlined in more detail in Sect. 2.1). For the most recent iterations of MOPITT products,
70 these a priori CO profiles are based on a monthly climatology from a chemical transport model. The degree
71 to which a given MOPITT retrieval reflects information obtained from the observed radiances – known as
72 “information content” – is highly spatially and temporally variable, depending on scene-specific factors such
73 as surface temperature, thermal contrast in the lower troposphere, and the actual (“true”) CO loading itself,
74 as well as on instrumental noise (e.g. Deeter et al., 2015). The lower the retrieval information content, the
75 closer the retrieved CO loading will be to the a priori; a model value.

76 Retrievals that take place over water are known to have a lower information content than retrievals
77 that take place over land. Primarily, this is due to weak thermal contrast near to the surface hampering the
78 instrument’s ability to sense CO absorption in the lowermost layers of the troposphere (Deeter et al., 2007;
79 Worden et al., 2010), and this is confounded by a lack of NIR reflectance over water, which limits these
80 retrievals to TIR wavelengths only. It is therefore recommended that MOPITT data users exclude these
81 retrievals from any analyses they perform, to ensure that results are not biased by retrievals that have a heavy
82 reliance on the a priori (MOPITT Algorithm Development Team, 2018; Deeter et al., 2015). Such filtering
83 is specifically emphasised where the focus of analysis is the identification of long-term CO trends, because
84 any real trends in the data will be weakened by the inclusion of retrievals that are tied heavily to the a priori
85 (Deeter et al., 2015). This is because the a priori CO profiles are taken from monthly modelled CO
86 climatologies: for a given location and day of the year, they will be the same every year and therefore feature
87 no temporal trend (Deeter et al., 2014).

88 MOPITT data are available as either Level 2 (“L2”) or Level 3 (“L3”) products. L2 products contain
89 each individual retrieval, at ~22 x 22 km spatial resolution. L3 products are a 1° x 1° gridded area-average of
90 the individual L2 retrievals that fall within each grid box (see Fig. 1), with some filtering criteria applied.
91 One criterion is the surface type over which the L2 retrievals were performed – either land, water, or “mixed”.
92 If more than 75 % of the bounded L2 retrievals were performed over the same surface type then only those
93 retrievals are averaged to create the L3 product and the rest are discarded; otherwise, all bounded L2 retrievals
94 are averaged, and the L3 product is given the surface type classification of “mixed” (L3 surface type
95 classification is explained in more detail in Sect. 2.2). This creates a problem for L3 grid boxes that overlay
96 coastlines: To a greater or lesser extent, these L3 products will have some contribution from L2 retrievals
97 performed over water, as shown in Fig. 1. L3 product users have limited capability to discard them, at least
98 without sacrificing temporal resolution, because each L3 grid box only has a single “retrieval” per day. By
99 contrast, with L2 products it is possible, for the same coastal grid boxes, to choose to retain only the retrievals
100 performed over land. In practical terms, this means that, for coastal L3 grid boxes, valuable retrieval
101 information over land, available in L2 products, can be lost to users of L3 products.

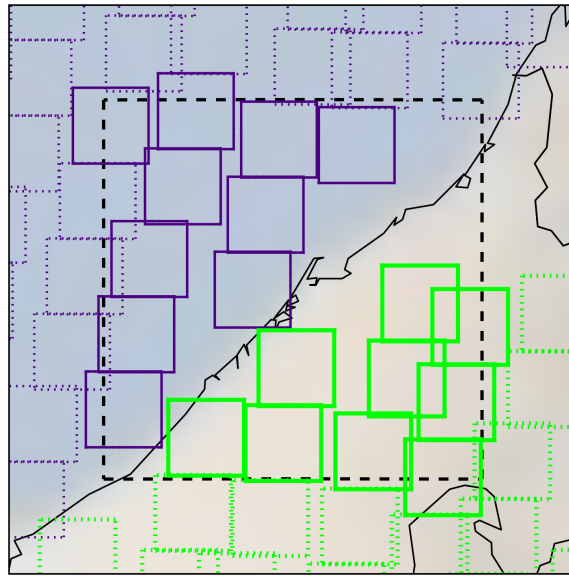


Figure 1. Example of a coastal L3 grid box (black dashed box) and bounded L2 retrievals from which the L3 products for that grid box are created. Purple (green) boxes correspond to L2 retrievals with a surface index of “water” (“land”). Note that only L2 retrievals with a midpoint that falls within the boundaries of the L3 grid box will be used in L3 creation for that grid box. These are indicated by solid purple/green outlines – those not included in L3 creation for this grid box are shown with dotted purple/green outlines. More information on surface indexing and L3 product creation is given in Sect. 2.2. “Coastal” L3 grid box classification is outlined in Sect. 2.3. The coastal L3 grid box visualized here contains the city of Dubai (~centre = 55.296° E, 25.277° N), which features in the case study analysis of Sect 3.4. Faint background shading is from Nasa Blue Marble imagery.

102 With a focus on the coastal L3 grid box containing the city of Halifax, Canada, Ashpole and Wiacek
 103 (2020) demonstrate the consequences of this loss of retrieval information in L3 products. They compare the
 104 results of analyses performed using L3 data and L2 data whereby only bounded retrievals performed over
 105 land were retained, and find significant differences in both seasonal mean statistics and the magnitudes of
 106 trends identified in surface-level CO. These differences are a direct result of the L3 products being dominated
 107 by L2 retrievals over water, which feature a weaker trend than the L2 retrievals over land, demonstrably due
 108 to a greater a priori influence owing to their reduced true-profile sensitivity. In their conclusions, Ashpole
 109 and Wiacek (2020) suggest that L2 retrievals over water should not contribute to L3 products for coastal grid
 110 boxes, which would be consistent with previous data filtering recommendations (MOPITT Algorithm
 111 Development Team, 2018; Deeter et al., 2015). The primary aim of this paper is to explore the extent of the
 112 difference that this would make on a global scale. This is necessary to understand for two reasons: firstly, L3
 113 data are more convenient for long time series analysis than L2 data owing to their smaller file size (~25 MB
 114 vs ~450 MB respectively, for a single daily, global file). It cannot be overlooked that working with L3 data
 115 thus requires fewer computing resources and less technical proficiency, with a range of simple-to-use tools

116 available for working with gridded products. L3 products thus make the MOPITT data more easily accessible,
117 especially to less-expert users, who may lack the expertise required to scrutinize the data for potential a priori
118 bias. Secondly, many of the world’s largest agglomerations are situated within a coastal L3 grid box (5 of
119 the top 10 and 33 of the top 100 largest agglomerations by population; derivation outlined in Sect. 2.5),
120 making these likely targets for analyses of air quality indicators, especially their changes over time.

121 This paper presents a comparison of results from analyses performed using original, “as downloaded”
122 L3 data products, and a new land-only L3 product (“L3L”, Ashpole and Wiacek (2022) – outlined in Sect.
123 2.4) that has been created from L2 products, for all MOPITT L3 grid boxes that overlay coastlines (a water-
124 only L3 product “L3W” has also been created for comparison purposes). Section 2 describes the datasets and
125 methods used, including outlining the creation of the new L3L and L3W data products analysed in this paper.
126 Section 3.1 demonstrates the magnitude of the sensitivity difference for retrievals over land and water,
127 zooming in to focus on coastal grid boxes (the classification of which is outlined in Sect. 2.3). Section 3.2
128 links the sensitivity contrast to differences in mean CO volume mixing ratios (“VMRs”) and their temporal
129 trends for L2 retrievals performed over land and water within coastal L3 grid boxes; and evaluates the effect
130 that the averaging together of these retrievals has on the statistics and trends in resulting L3 “mixed” values.
131 Section 3.3 quantifies the proportion of L2 retrievals performed over land within coastal L3 grid boxes that
132 are lost to L3 products, before finally comparing statistics and trends in L3 and L2 products for all coastal
133 L3 grid boxes, outlining the magnitude and significance of differences for the coastal grid boxes that contain
134 33 of the largest 100 cities in the world (Sect. 3.4).

135

136

137 **2. Data and Methods**

138

139 **2.1. MOPITT Instrument and retrieval overview**

140

141 Carried on board the polar-orbiting NASA Terra satellite that was launched in December 1999, MOPITT
142 began measuring CO in March 2000 and has provided near-continuous measurements to date. With a native
143 pixel resolution of ~22 x 22 km at nadir and a swath width of ~640 km, it offers near global coverage roughly
144 every 3-days, crossing the equator at ~10:30 and ~22:30 local time. The instrument is a gas correlation
145 radiometer that measures radiances in two CO-sensitive spectral bands: the TIR at 4.7 μm , which is sensitive
146 to both absorption and emission by CO and can provide information on its vertical distribution in the
147 troposphere; and the NIR at 2.3 μm , which constrains the CO total column amount and yields information
148 on CO concentrations in the lower troposphere (LT), to which TIR radiances are typically less sensitive

149 (Drummond et al., 2010; Pan et al., 1995, 1998). For the work presented here, the TIR-NIR combined
150 MOPITT product is used, owing to its demonstrably greater sensitivity to CO loadings near to the surface
151 than the TIR- and NIR- only products which are also available (Deeter et al., 2013). Note, however, that
152 retrievals over water and at night are limited to the TIR band only due to the lacking NIR signal. This analysis
153 is based on daytime-only retrievals (more information on data selection and preparation is given in Sect. 2.4).

154 Multiple other sources describe the retrieval algorithm in detail (e.g., Deeter et al., 2003; Francis et
155 al., 2017). In short, it uses optimal estimation (Pan et al., 1998; Rogers, 2000) and a fast radiative transfer
156 model (Edwards et al., 1999) to invert measured radiances and retrieve the CO volume mixing ratio (VMR)
157 profile on 10 vertical layers. The vertical grid consists of 9 equally spaced pressure levels from 900 to 100
158 hPa (the uppermost level covers the atmospheric layer from 100 to 50 hPa), with a floating surface pressure
159 level (if the surface pressure is below 900 hPa, less than 10 profile levels are retrieved). Retrieved values
160 represent the mean CO VMR in the layer immediately above that level. These profile measurements are then
161 integrated to provide total column CO amounts. Retrievals are only performed for scenes free of cloud (cloud
162 clearing is based on coincident MODIS observations and MOPITT's own radiances).

163 In addition to the measured radiances, the retrieval requires multiple inputs including meteorological
164 data, surface temperature and emissivity, and, of direct relevance to this study, a priori CO profiles, which
165 are necessary to constrain the retrieval to physically reasonable limits. These a priori CO profiles come from
166 a monthly CO climatology (years 2000-2009), simulated with the Community Atmosphere Model with
167 Chemistry (CAM-chem) chemical transport model (Lamarque et al., 2012) at a spatial resolution of $1.9^\circ \times$
168 2.5° , which is then spatially and temporally interpolated to the time and location of each individual MOPITT
169 observation. A priori profiles for a given location and day of the year are therefore the same every year and
170 feature no temporal trend. To understand the physical significance of the MOPITT CO retrievals, it is
171 necessary to examine the retrieval Averaging Kernels (AKs), available with all MOPITT data products,
172 which quantify the sensitivity of the retrieved vertical profile to the "true" vertical profile. The lower the
173 retrieval sensitivity, the greater the a priori weighting. Two different components of AKs are analysed in this
174 paper: AK rowsums, which represent the overall sensitivity of the retrieved profile at the corresponding
175 pressure level to the whole true profile; and AK diagonal values, which represent the sensitivity of the
176 retrieved profile at the corresponding pressure level to the same level of the true profile (e.g. the AK diagonal
177 value for the surface level of the retrieved profile represents its sensitivity to the surface level of the true
178 profile).

179 From time-to-time, new MOPITT products become available as improvements are made to the
180 retrieval algorithm and radiative transfer model, yielding superior validation statistics compared to earlier
181 product versions (Worden et al., 2014). This analysis uses MOPITT Version 8 (V8) products (Deeter et al.,

182 2019). Note that Version 9 (V9) products became available shortly after this study was completed. V9
183 features cloud screening improvements that yield additional retrievals over land in comparison to V8 (the
184 exact percent change varies significantly with geography). Validation results are comparable to V8. An
185 overview of MOPITT V9 is given by Deeter et al (2022). A subset of the analysis presented in this paper has
186 been duplicated using V9 data, and this confirms that the main conclusions drawn based on V8 data also hold
187 for V9 (this analysis is outlined in the Supp. Mat. (SM1)). This is to be expected, given that the land-water
188 sensitivity contrast remains in V9 and the L3 processing method is unchanged.

189
190

191 **2.2. MOPITT surface type classification**

192

193 To aid in filtering and interpreting retrievals, all MOPITT data products are distributed with a range of
194 diagnostic fields. As retrieval information content is known to be variable depending on the type of surface
195 over which it is performed (Deeter et al., 2007), L2 retrievals are given a surface index according to whether
196 they were performed over land, water, or a combination of the two (“mixed”). For a given 1° x 1° L3 grid
197 box, how the L2 retrievals that fall within its boundaries are processed to produce the L3 product depends on
198 how their surface indexes vary: If more than 75 % of the bounded L2 retrievals have the same surface index,
199 only those retrievals are averaged to produce the L3 gridded value, and the L3 surface index is set to that
200 surface type (the other L2 retrievals are discarded). Otherwise, all L2 retrievals available in the L3 grid box
201 are averaged together and the L3 surface index is set to “mixed”, as is the case in the example shown in Fig.
202 1 (this information is taken from the MOPITT Version 6 L3 data quality summary¹, which at the time of
203 writing, is the most recent data quality summary to detail exactly how L3 data are created, despite more
204 recent data quality summaries being available). Note that the L2 VMR profiles that are averaged to produce
205 the L3 retrieval are first converted to log(VMR) profiles, then averaged, and the mean log(VMR) profile is
206 then converted back to a VMR profile.

207 Each L3 grid box only has one retrieval per day. This dictates that where the grid box overlies both
208 land and water, its surface index could vary through time, depending on the population of L2 retrievals from
209 which it is created. The make-up of this population can also vary from day-to-day due to factors such as cloud
210 cover, and screening for data quality issues: on day n the population could be predominantly L2 retrievals
211 over land, on day $n+1$ it could be predominantly L2 retrievals over water, and on day $n+2$ it could be an even
212 mix of the two. Given that the averaging together of retrievals with significantly different sensitivity profiles
213 – as could be the case when averaging retrievals over land and water – serves to dilute the information coming

¹ available here: https://eosweb.larc.nasa.gov/sites/default/files/project/mopitt/quality_summaries/mopitt_level3_ver6.pdf

214 from the MOPITT observed radiances with information coming from the a priori and is therefore discouraged
215 (MOPITT Algorithm Development Team, 2018; Deeter et al., 2015; Deeter et al., 2007); and that MOPITT
216 data users are advised to exclude retrievals over water from analyses owing to the known reduced sensitivity,
217 this introduces two potential problems for L3 data taken from coastal grid boxes: firstly, discarding all L3
218 retrievals with the surface index of water will result in a loss of temporal coverage; secondly, L3 retrievals
219 with a surface index of mixed feature some contribution from L2 retrievals over water. The consequences of
220 both these problems are explored in this paper.

221
222

223 **2.3. Coastal grid box classification for this study**

224

225 Since the focus of this paper is on “coastal” L3 grid boxes, it is first necessary to isolate these from the
226 remaining “land-only” or “water-only” L3 grid boxes in the MOPITT data set. The initial step is to identify
227 all grid boxes that have a surface index of “mixed” at least once during the study period. This indicates that
228 the ground area within those grid boxes was both land and water. However, analysis of the global distribution
229 of L3 grid boxes featuring a surface index of mixed revealed that, in addition to actual coastlines, a large
230 proportion of inland grid boxes that are clearly not coastal (“false coastal”) are given the surface index of
231 mixed at least some of the time (Fig. 2a). The reason for this is unclear, but it could be for real physical
232 reasons, such as land grid boxes sporadically flooding, or due to issues in the retrieval schemes caused by
233 e.g. cloud screening problems or the presence of surface ice cover. One characteristic of these false coastal
234 grid boxes is that, compared to the total number of days with L3, the relative frequency with which they are
235 flagged as land is very high (expressed as the ratio “n_days(L3O_L/L3O)”, plotted in Fig. 2b). This relative
236 frequency is much lower for “true” coastal grid boxes, to be expected given prior knowledge of 1) the fact
237 that these grid boxes span both land and water surface types; and 2) how the surface index is determined for
238 L3 data (as outlined in Sect. 2.2). Following iterative threshold testing, L3 coastal grid boxes are classified
239 as grid boxes that:

240

- 241 1. Have at least one classification of “mixed” during the study period
- 242 2. Have an n_days(L3O_L/L3O) ratio < 0.5.

243

244 The distribution of coastal grid boxes identified using these criteria is shown in Fig. 2c. Most false coastal
245 grid boxes are removed, although there are still some erroneous classifications evident, mostly in the north
246 of Canada and Russia. However, placing a more restrictive threshold on the n_days(L3O_L/L3O) ratio to

247 remove these areas has diminishing returns since it results in the rejection of more true coastal grid boxes.
248 These criteria therefore strike a balance between minimising false and maximising true classifications.

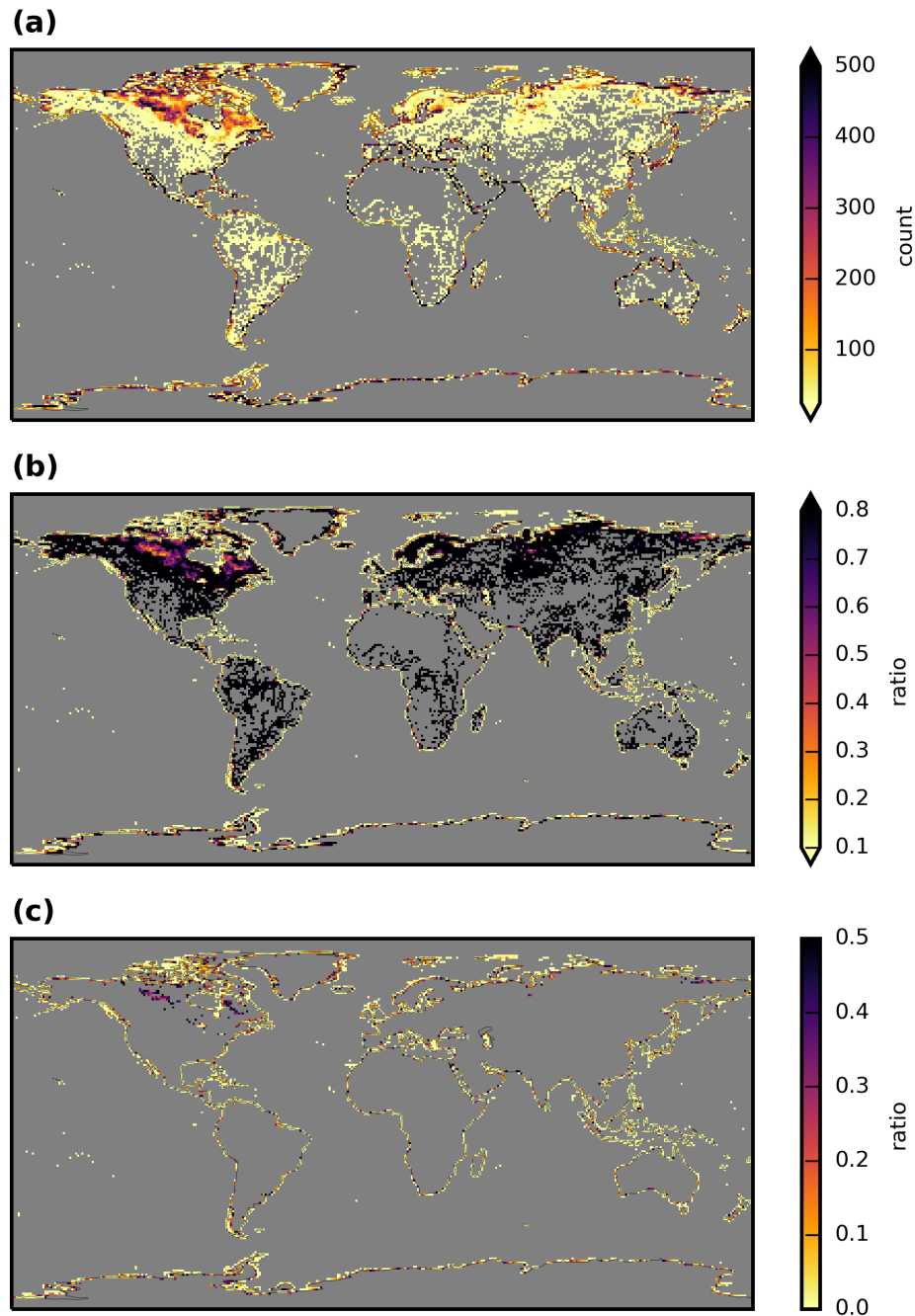


Figure 2. Maps showing the stages of derivation of the coastal L3 grid box mask applied in this paper to MOPITT data. **(a)** Frequency with which L3 grid boxes are given the surface index of “mixed”, calculated from daily data between 2001-08-25 and 2019-02-28. **(b)** Frequency with which L3 grid boxes that have a surface index of “mixed” at least once in panel a have the surface index of “land”, compared to the total number of days with which L3 data are available for that grid box (expressed as $n_days(L3O_L/L3O)$). **(c)** As b, but with a threshold of $n_days(L3O_L/L3O) < 0.5$ applied. This is the coastal L3 grid box mask used in this paper.

249 Applying these criteria to the MOPITT L3 data yields 4299 coastal grid boxes, from a total of 64800
250 L3 grid boxes (6.6 %). This mask is applied to all data, and only those L3 grid boxes that remain are classified
251 as coastal. Only data for these coastal grid boxes are analysed in this study (with the exception of global L3
252 maps analysed in Sect. 3.1.1).

253
254

255 **2.4. MOPITT datasets analysed, and data processing method for creating land- and water-only L3** 256 **products (“L3L” and “L3W”)**

257

258 All available MOPITT V8 Level 2 (L2) and Level 3 (L3) daily TIR-NIR files (“MOP02J” and “MOP03J”
259 files, respectively) were downloaded from the NASA Earthdata portal (<https://search.earthdata.nasa.gov>).
260 Although the data record begins in March 2000, analysis is restricted to the period from 2001-08-25 to 2019-
261 02-28. Data prior to 2001-08-25 are discarded due to an instrumental reconfiguration in 2001 creating an
262 inconsistency in the data record (Drummond et al., 2010). Data post 2019-02-28 are flagged as “beta” at the
263 time of writing, their use in scientific analysis (especially for examining long-term records of CO) being
264 discouraged until final processing and calibration occurs (MOPITT Algorithm Development Team, 2018).
265 For clarity, the original, “as-downloaded” L3 time series is referred to as “L3O” for the remainder of this
266 paper. Only retrievals that were performed during daytime hours are retained (daytime and nighttime
267 retrievals are stored as separate fields in MOP03J files). For this analysis, separate subsets of L3O are created
268 according to surface index: L3O land-only (“L3OL”), L3O water-only (“L3OW”), L3O mixed (“L3OM”), L3O
269 land-or-mixed (“L3OLM”). When the L3O dataset is analysed with no filtering by surface index applied, it is
270 referred to as “L3ONF”.

271 The land- and water-only L3 products are created from daily L2 data. The first step of L2 data
272 processing required is to filter the retrievals as is done for the processing of L3O. This involves:

273

- 274 • Discarding all observations for Pixel 3 (this corresponds to one of MOPITT’s four detectors);
- 275 • Discarding all observations where both (1) the channel 5A signal-to-noise-ratio (“SNR”) < 1000 and
276 (2) the channel 6A SNR < 400 (5A and 6A correspond to the average radiances for MOPITT’s length-
277 modulated cell TIR and NIR channels, respectively)

278

279 This filtering takes place because observations from specific elements on MOPITT’s detector array were
280 found to exhibit greater retrieval noise than the other elements, and their inclusion therefore lowered overall

281 L3 information content (MOPITT Algorithm Development Team, 2018). Only daytime L2 retrievals are
282 retained, using a solar zenith angle filter of $< 80^\circ$.

283 From the remaining set of filtered L2 retrievals, separate area averages are taken for those with a
284 surface index of land and water, for every $1^\circ \times 1^\circ$ L3 grid box. This effectively creates two new L3 “land-
285 only” and “water-only” products, which are referred to herein as “L3L” and “L3W”. For clarity of analysis,
286 remaining L2 retrievals with a surface index of mixed are discarded. These make up a very small proportion
287 of the overall L2 retrievals (e.g. $< 5\%$ for the grid box containing Halifax, analysed in Ashpole and Wiacek,
288 2020). Both L3L and L3W are publicly available for download (Ashpole and Wiacek, 2022). Note that, as
289 with the creation of L3O, L2 VMR profiles for each L3 grid box are first converted to $\log(\text{VMR})$ profiles
290 before averaging, and the mean $\log(\text{VMR})$ profile is then converted back to a VMR profile to give the final
291 L3L and L3W retrievals. Additionally, the number of L2 retrievals that are used for calculating the area
292 averages when creating L3L and L3W (“ n_{ret_L} ” and “ n_{ret_W} ”, respectively) is recorded. The ratio
293 $n_{\text{ret}_L}/n_{\text{ret}_W}$ (herein referred to as “ratio(land/water)” for simplicity) is used to indicate the proportion of
294 the L3 grid box that is covered by land vs water: a ratio of 1 indicates an even split of these surface types in
295 the grid box; a ratio < 1 indicates that a greater proportion of its surface is water covered; and a ratio > 1
296 indicates that the grid box is land-dominated.

297 From the L3O, L3L, and L3W datasets, only grid boxes that are classified as “coastal” using the
298 coastal grid box masked outlined in Sect. 2.3 are analysed.

299 Note that the analysis presented in this paper is restricted to daily products. Monthly L3 files are
300 available, however the absence of a monthly L2 product precludes the analysis from being conducted on
301 those data. Based on the results of the analysis of daily data, however, there is reason to also advise caution
302 if working with coastal grid boxes in the monthly L3 product. This is because the data for those grid boxes
303 will still be created from daily L2 retrievals over land and water, with the same implications that are discussed
304 in this paper.

305

306

307 **2.5. Time series preparation, statistical methods, and additional data sources**

308

309 For every coastal L3 grid box, two separate time series from each of the L3O, L3L, and L3W datasets are
310 analysed:

311

- 312 1. The time series analysed in Sect. 3.1 and 3.2 only contain days where L3L and L3W are both present
313 and the L3O surface index is mixed (“L3O_M”). This is to ensure that the true CO profiles are as similar

314 as possible when directly comparing L3L and L3W for a given coastal grid box. Furthermore, it
315 allows for the analysis of the resulting L3O_M data on these days with knowledge of the parent L2
316 retrievals over land and water and their differences.

- 317
- 318 2. In Sect. 3.3 and 3.4 the full time series from each dataset is analysed with no temporal filtering
319 applied.

320

321 Descriptive statistics are calculated from both time series across the whole study time period, and also
322 for individual years (full years only – 2002 to 2018 inclusive) in order to perform the regression analysis
323 outlined below.

324 To identify and compare temporal trends for each coastal grid box in the datasets outlined above,
325 weighted least squares (WLS) regression analyses is performed on yearly mean values, weighted by the
326 inverse of the standard deviation of the measurements used in the yearly mean (i.e. $1/\sigma$). For years that contain
327 just a single retrieval, the weighting is set to $1/100000$ to de-weight them in the fit. If there are more than 2
328 years in a time series for a given grid box that have no data, the regression analysis is not performed. WLS
329 is preferred over OLS because it is less sensitive to outliers. For simplicity, no other trend detection methods
330 – e.g. the Thiel-Sen slope estimator – are applied to corroborate the trends that are detected with WLS, nor
331 do we analyse additional datasets to verify them. Such extra steps would be necessary if the actual trend
332 values were the focus of this study; however, the aim of this trend analysis is instead to identify whether the
333 same method can yield different results depending on which of L3O, L3L or L3W is analysed. Trend
334 verification is beyond the scope of this study.

335 To determine whether two trends identified are significantly different, their difference is evaluated
336 using the Z test as follows:

337

$$338 Z = \frac{Trend_1 - Trend_2}{\sqrt{SE_1^2 + SE_2^2}}$$

339

340 where SE_1 and SE_2 correspond to the standard errors of $Trend_1$ and $Trend_2$ respectively, and Z is the test
341 statistic. Where Z is greater (less) than 1.645 (-1.645) the trend difference is statistically significant to at least
342 90 % (i.e. $p < 0.1$). In addition, two trends are classified as being significantly different if $Trend_1$ is
343 significantly different to zero ($p < 0.1$) but $Trend_2$ is not ($p > 0.1$), and vice-versa (i.e. the conclusion would
344 be that $Trend_1$ is not zero, but $Trend_2$ may be).

345 A list of the top 100 largest agglomerations by population in the world is obtained from
346 <http://www.citypopulation.de/> (valid at time of writing). 33 of these are situated in a coastal grid box,
347 according to the classification in Sect. 2.3. Time series of L3L, L3W, and L3O are extracted from each of
348 these grid boxes for the analysis in Sect. 3.4.

349
350

351 **3. Results and Discussion**

352

353 **3.1. Land-water contrast in MOPITT sensitivity**

354

355 This section demonstrates the land-water sensitivity contrast in MOPITT retrievals at levels throughout the
356 vertical profile, and examines the magnitude of the difference within coastal L3 grid boxes.

357

358

359 **3.1.1. Global context**

360

361 Figure 3 shows long-term mean maps for the retrieval sensitivity metrics AK diagonal value, AK rowsum,
362 and retrieved minus a priori VMR (“VMR ret-apr”) at selected profile levels, created from L3O data averaged
363 across the entire study period (September 2001 – February 2019, inclusive). All indicators show that retrieval
364 sensitivity is greater over land than water in the lower troposphere (“LT”; represented by the surface, 900
365 hPa and 800 hPa profile levels), with sharp differences evident at almost all land-water boundaries. The
366 sensitivity contrast clearly decreases in strength with height. By mid-tropospheric levels (“MT”; represented
367 by 600 hPa profile level), AK diagonal values and rowsums reach greater values on average over water than
368 land. Some strong land-water gradients remain present in VMR ret-apr fields, most notably over North
369 Africa, the Arabian peninsula, and south-east China, but on average these values are much more similar
370 across land and water than in the LT. No clear land-water contrast is evident in the upper troposphere (“UT”;
371 represented by the 300 hPa profile level), with retrieval sensitivity instead varying more with latitude,
372 decreasing towards both poles (a companion to Fig. 3 with an altered colour bar to better show spatial patterns
373 in AK diagonal values and rowsums at MT and UT levels is provided in the Supp. Mat. (SM2)).

374 AK diagonal values and rowsums show that retrieval sensitivity increases across both land and water
375 with height. It is lowest at the surface level, with little information content in the retrieval over water (AK
376 diagonal values and rowsums over water are less than half what they are over land, on average). There is high
377 spatial variability over land: AK diagonal values and rowsums reach values comparable to those at higher

378 profile levels in some sensitivity hotspots (e.g. parts of central Europe, east Asia, eastern USA and tropical
 379 west Africa), while being more comparable to values over water in other areas. By 800 hPa, AK diagonals
 380 and rowsums over water reach values comparable to or greater than those reached over land at the surface
 381 level, in most places.
 382

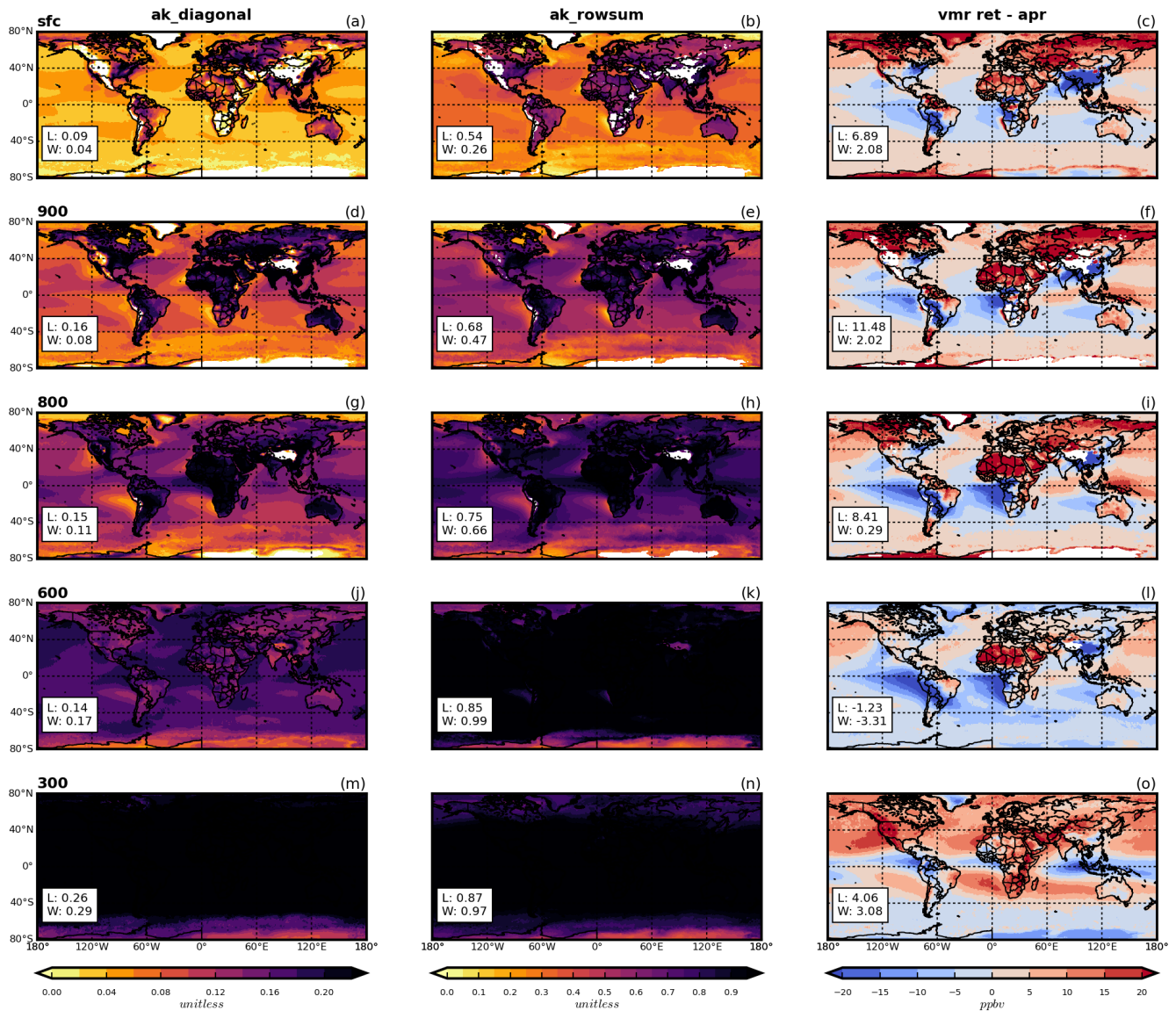


Figure 3. Mean sensitivity metrics from MOPITT L3 data, averaged across the entire study period (September 2001 – February 2019, inclusive). Shown are AK diagonal values (left column), AK rowsums (center column) and VMR retrieved minus a priori values (right column) for the following levels of the retrieved profile: surface (top row), 900 hPa (second row), 800 hPa (third row), 600 hPa (fourth row), and 300 hPa (bottom row). Values in white boxes correspond to mean values across all land (“L”) and water (“W”) L3 grid boxes.

383 Spatial patterns in retrieved minus a priori VMRs are slightly more complex to interpret, because they
384 are influenced both by retrieval sensitivity and the accuracy of the a priori. For example, while VMR ret-apr
385 values close to zero can indicate a retrieval that is heavily weighted by the a priori and therefore low retrieval
386 sensitivity, they can also indicate that the true VMR is close to the a priori value. Despite this, retrieved minus
387 a priori VMR values clearly reach more strongly positive or negative values over land than water in the LT,
388 with the contrast becoming less pronounced with height. Furthermore, there are clear land-water
389 changepoints in the LT. This further demonstrates the impact of the land-water contrast in retrieval
390 sensitivity.

391

392

393 **3.1.2. Analysis of coastal L3 grid boxes**

394

395 Scatterplots of sensitivity metrics at selected profile levels, for coastal L3 grid boxes only, are shown in Fig.
396 4. Specifically, these plots show the sensitivity of the L2 land and water retrievals that are bounded by the 1°
397 x 1° L3 grid boxes and used to create the L3O data. The values that are plotted correspond to the long-term
398 mean from the L3L and L3W datasets for these grid boxes.

399 The AK diagonal value and rowsum plots clearly demonstrate greater sensitivity over land (L3L) than
400 over water (L3W) at LT levels (a point below the diagonal line on these panels indicates greater values in
401 L3L) for the majority of grid boxes, with the difference decreasing into the MT and UT. Correspondingly,
402 retrieved VMRs also deviate more greatly from their a priori values in L3L than L3W in the LT, with smaller
403 land-water differences in the MT and UT. Mean values are significantly different ($p < 0.005$) apart from AK
404 diagonal values and retrieved minus a priori VMR at 300 hPa ($p = 0.13$ and 0.07 respectively). Sensitivity
405 metrics are generally better correlated in the MT and UT than at LT levels.

406 This analysis clearly shows how L2 retrievals that are averaged together to create the L3O data over
407 coastal grid boxes have differing degrees of sensitivity, especially in the LT. This is explicitly cautioned
408 against in the MOPITT data user's guide (MOPITT Algorithm Development Team, 2018). The remainder of
409 this paper focuses on the surface-level of the retrieved profile, since the LT is where discrepancies are
410 greatest, and the cause of this sensitivity disparity is well established: differing thermal contrast conditions
411 near to the surface over land and water; and a lack of NIR radiances being used in the retrieval over water.
412 Furthermore, the surface-level is of most interest for identifying potential air quality impacts for humans (e.g.
413 Buchholz et al., 2022).

414

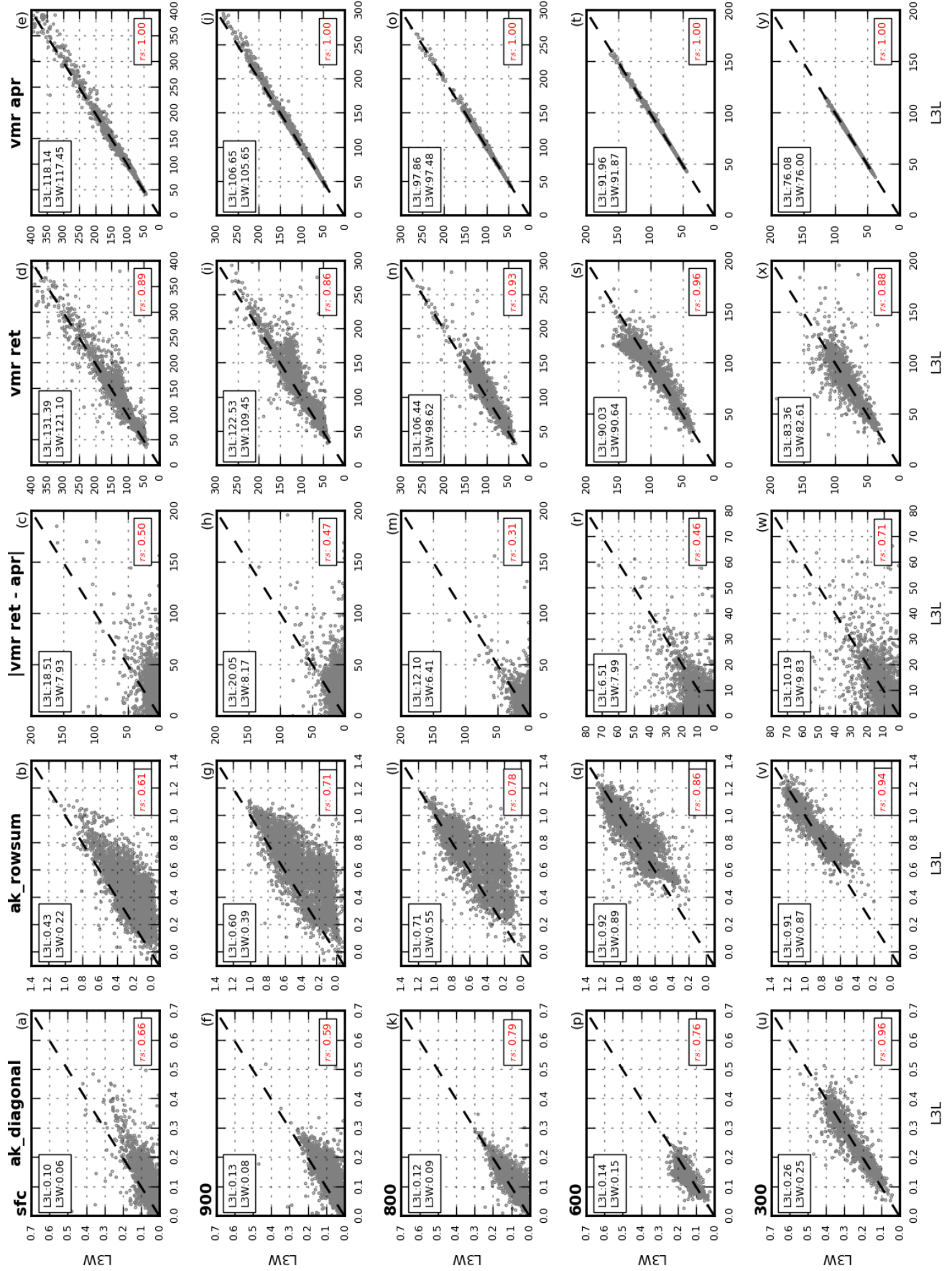


Figure 4. Mean sensitivity metrics and VMRs (retrieved and a priori) from coastal L3 grid boxes. Values compared in the scatterplots are mean values from matched L3L and L3W retrievals within these grid boxes. “Matched” means that only days when both L3L and L3W are present, and the L3O surface index is mixed, are used to create the mean values analysed. Shown are AK diagonal values (left column), AK rowsums (second column), absolute VMR retrieved minus a priori values¹ (third column), retrieved (fourth column) and a priori (fifth column) VMRs, for the following levels of the retrieved profile: surface (top row), 900 hPa (second row), 800 hPa (third row), 600 hPa (fourth row), and 300 hPa (bottom row). Values in boxes in the top-left corner of each panel correspond to mean values across all L3L and L3W grid boxes. These means are significantly different using a 2-tailed t-test (unequal variance) with $p < 0.005$ in all cases except `ak_diagonal` at 300 hPa where $p = 0.13$, `vmr_ret_minus_apr` at 300 hPa where $p = 0.07$, `vmr_ret` at 600hPa where $p = 0.30$, `vmr_ret` at 300hPa where $p = 0.11$. No `vmr_apr` mean differences are significant. Values in the bottom-right corner of each panel correspond to the Spearman’s rank correlation coefficient ($p < 0.005$ in all cases).

¹ Note that for ease of interpretation, the absolute retrieved minus a priori VMR values are plotted, i.e. ignoring whether the result is positive or negative. However, the results hold if using signed values, and a duplicate of Fig. 4 with signed retrieved minus a priori VMR values is included in the Supp. Mat. for reference (SM3).

416

417

418

419 **3.2. Differences in retrieved VMRs and temporal trends, and their relation to the land-water sensitivity**

420 **contrast**

421

422 **3.2.1. L3L vs L3W**

423

424 *Retrieved VMR comparison between L3L and L3W*

425

426 In addition to the clear land-water LT sensitivity contrast in coastal grid boxes, there are clear differences in
427 the retrieved VMRs (Fig. 4; Fig. 5a (black boxplots)). The retrievals performed over land yield surface-level
428 VMRs that are over 10 ppbv greater than over water, on average. As with sensitivity, land-water differences
429 in retrieved VMRs decrease higher up in the profile.

430

431 Greater land-water sensitivity differences also tend to be associated with greater retrieved VMR
432 differences. Figure 5b shows the distribution of retrieved surface level VMR differences ($L3L - L3W$)
433 stratified by the corresponding surface level AK rowsum difference. Larger retrieved VMR differences are
434 clearly associated with greater AK rowsum differences (some degree of spread in the results is expected,
since the relationship also depends on the accuracy of the a priori, as outlined previously).

435

436 Of the 3971 coastal grid boxes that are compared, 60 % (2379) show a significant difference ($p < 0.1$,
determined using a 2-tailed student’s t-test) in mean VMRs in L3L and L3W (Fig. 5a). Compared to grid
437 boxes where the mean VMR difference is not significant, there are several notable differences (detailed in
438 Table 1). As expected from the previous analysis, the land-water sensitivity contrast is greater when mean
439 VMRs are significantly different (“SIGDIFF”) than when not (“NOT_SIGDIFF”). This is evident in AK
440 rowsum and VMR retrieved minus a priori differences (the magnitude of difference between subsets is around

441 50 % and 100 %, respectively). Interestingly, the AK difference is due to sensitivity being lower over water
442 in SIGDIFF than in NOT_SIGDIFF; sensitivity over land is similar in both subsets. This may be explained
443 as follows: when sensitivity over water is especially low, as is the case in SIGDIFF, the retrieved VMR will
444 be heavily weighted by the a priori and unable to match the variation present in the more sensitive retrieval
445 over land. As sensitivity over water increases, this a priori weighting weakens and the retrieved VMR will
446 more closely track the retrieval over land, resulting in a less significant difference. Also of note, a priori
447 VMRs are much lower in SIGDIFF than in NOT_SIGDIFF, on average. Considered alongside the greater
448 retrieved minus a priori differences, this suggests that the a priori VMR could be a less accurate estimate of
449 the “true” VMR for the SIGDIFF subset, whereas it is closer to reality for the NOT_SIGDIFF subset.
450 Intuitively, this makes sense: for a hypothetical situation where the a priori VMR is a perfect match for the
451 “true” VMR, and both are uniform across a coastal L3 grid box, retrievals over the land and water portions
452 of the grid box would be expected to be identical irrespective of any differences in retrieval sensitivity over
453 those surfaces. To summarise: assuming “true” VMRs are similar over land and water within coastal L3 grid
454 boxes, differences in retrieved VMRs depend not only on the sensitivity of the retrieval, but also on the
455 accuracy of a priori VMRs used in the retrievals.

456 It should be noted that there are additional physical factors that could plausibly play a role in
457 generating the L3L – L3W retrieved VMR difference that is observed, in addition to retrieval sensitivity.
458 Given that most CO sources are land-based, a decrease in VMRs from land to water might be expected,
459 especially in the LT. However, this assumption only seems reasonable where large CO sources are proximal
460 to the coastline, as it is unrealistic to expect gradients as large as we observe in background CO (which coastal
461 grid boxes far from large CO sources are more likely to represent) across the relatively small distance covered
462 by a L3 grid box. Given the relatively long-lived, well-mixed nature of atmospheric CO, VMRs retrieved at
463 a given location are a function of both local emissions *and* transport, and the portion of coastal L3 grid boxes
464 situated over water therefore do not represent pristine conditions in comparison to the adjacent land-based
465 portion of the grid boxes. This is verified by comparing a priori VMRs (also shown in Figure 4), which
466 suggest the land-water difference in CO concentrations should be negligible (mean L3L – L3W a priori VMR
467 difference = 0.69 ppbv, compared to a mean retrieved VMR difference of 10.29 ppbv). The above reasoning
468 can also be applied to the question of whether wind direction is responsible for creating the observed L3L –
469 L3W difference in retrieved VMRs: It could be hypothesised that a prevailing onshore wind may lead to CO
470 concentrations being higher over land than water, yet the negligible L3L – L3W a priori VMR difference,
471 the fact that atmospheric CO is well-mixed, and the clear land-water sensitivity gradient that has been
472 demonstrated suggest that wind direction does not play a big role in creating the land-water difference
473 observed in retrieved VMRs. To further rule out the role of wind direction, the L3L – L3W retrieved VMR

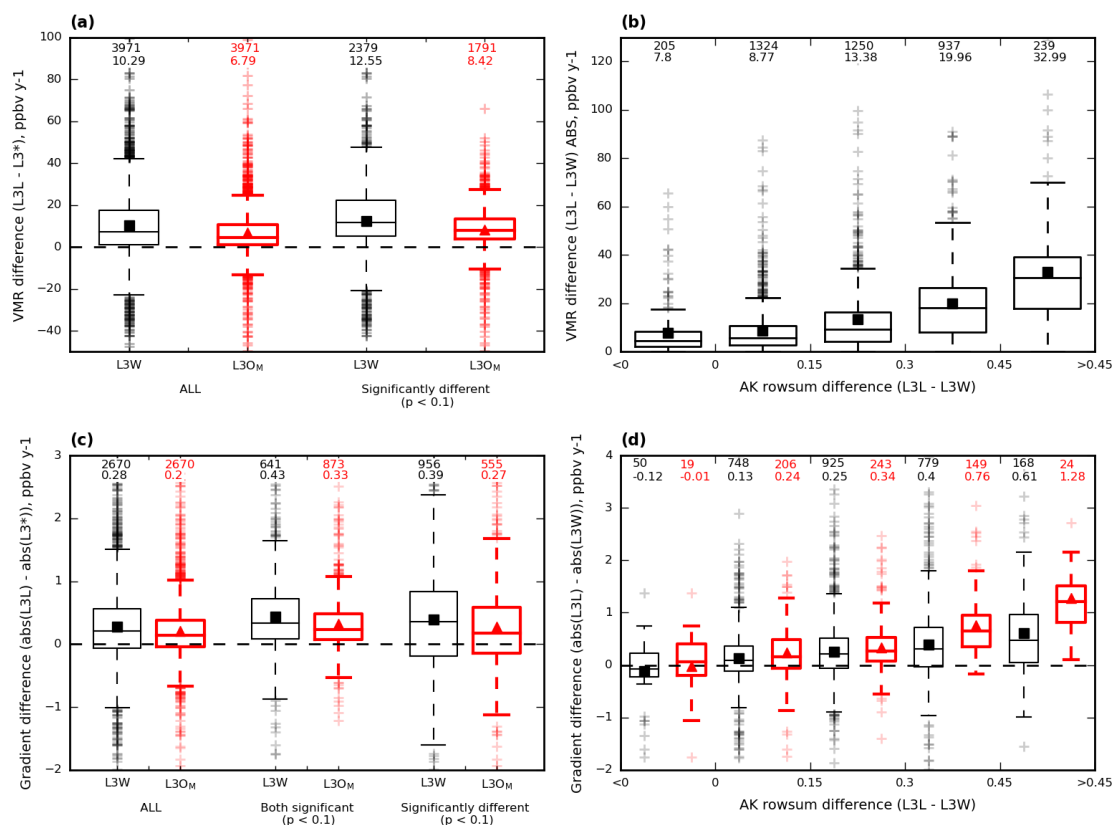


Figure 5. Boxplots showing how mean VMRs and trends from WLS analysis compare for coastal L3 grid boxes, calculated from matched retrievals within these grid boxes. “Matched” means that only days when both L3L and L3W are present and the L3O surface index is mixed are used to create the mean values analysed. Mean values are represented by filled squares/triangles, and values above the boxplots correspond to number of grid boxes with data for that boxplot, and the mean value, respectively. **(a)** Mean VMR differences for L3W (black, mean values represented by filled squares) and L3O_M (red, thicker lines, mean values represented by filled triangles) compared to L3L (L3L - L3* in both cases). Shown are the differences for all coastal grid boxes, and only for those grid boxes where the difference is significant ($p < 0.1$), determined using a 2-tailed t-test. **(b)** Absolute mean VMR differences¹ between L3L and L3W, stratified according to corresponding AK rowsum difference (L3L - L3W in both cases). **(c)** Absolute differences in gradients² detected using WLS regression analysis for L3W (black, mean values represented by filled squares) and L3O_M (red, thicker lines, mean values represented by filled triangles), compared to L3L (L3L - L3* in both cases). Shown are differences for all coastal grid boxes where WLS analysis could be performed, for grid boxes where both trends compared are significantly different to zero ($p < 0.1$), and for grid boxes where the trend difference is significant ($p < 0.1$). **(d)** Absolute differences in gradients² detected using WLS regression analysis between L3L and L3W, stratified according to corresponding AK rowsum difference (L3L - L3W in both cases). Shown are the differences for all coastal grid boxes where WLS could be performed (black, mean values represented by filled squares), and only for those grid boxes where the detected trend is significant ($p < 0.1$) in both L3L and L3W (red, thicker lines, mean values represented by filled triangles).

¹Absolute retrieved VMR difference values are shown in Fig. 5b for clarity, since L3L - L3W can be either positive or negative depending on whether a priori VMRs used in the retrieval are greater or less than the “true” VMR being retrieved, which complicates the analysis. The corresponding plot with raw values (i.e. not discarding the +/- sign) is included in the Supp. Mat. however, and the same conclusions can be drawn based on this figure (SM4).

²For clarity, differences between the absolute trend values (i.e. ignoring the +/- sign of the trend) are presented, since this shows the degree of difference in the trend magnitude, irrespective of trend direction. A positive trend difference in this case signifies a stronger (faster) trend in L3L than L3* (panel c) or L3W (panel d).

Table 1. Mean values for selected variables from L3L and L3W for coastal L3 grid boxes, matched retrievals only. “Matched” means that only days when both L3L and L3W are present and the L3O surface index are mixed are used to create the mean values analysed. Mean values are calculated and presented separately according to the results of a 2-tailed student’s t-test (unequal variance) performed on mean retrieved VMR values in L3L and L3W (n = 3971). Mean L3L – L3W differences are also shown for each subset (‘L-W’)

	P < 0.1 (“SIGDIFF”) (n=2379, 60 %)			P > 0.1 (“NOT_SIGDIFF”) (n=1592, 40 %)		
	L3L	L3W	L-W	L3L	L3W	L-W
Mean vmr_ret	129.97	117.41	12.55	133.52	126.60	6.90
Mean vmr_apr	113.78	113.18	0.61	124.65	123.83	0.83
Mean ret-apr	16.18	4.24	11.94	8.87	2.77	6.09
Mean ak rowsum	0.43	0.18	0.24	0.44	0.27	0.16

475 comparison has been analysed alongside wind direction for several case study grid boxes, and there appears
 476 to be no notable shift in wind direction whether L3L or L3W is greater for a given grid box. Results for this
 477 analysis are given in the Supp. Mat. (SM5). The weight of evidence therefore points towards L3L – L3W
 478 retrieved VMR differences being a function of reduced retrieval sensitivity over water compared to land.

479

480 *Trend comparison between L3L and L3W*

481

482 We now compare temporal trends detected in L3L and L3W for coastal grid boxes, and relate differences to
 483 the land-water sensitivity contrast outlined previously.

484 On average, across all grid boxes where WLS can be performed in both datasets following the criteria
 485 outlined in Sect. 2.5 (n = 2670), trends are stronger in L3L than L3W (Fig. 5c (black boxplots)), with the
 486 range of differences around 2.5 ppbv y⁻¹ (~-1 ppbv y⁻¹ to 1.5 ppbv y⁻¹). When the comparison is restricted to
 487 grid boxes where both trends are significantly different to zero (p < 0.1; 641 of the 2670 grid boxes, 24 %),
 488 a greater proportion of those grid boxes have a stronger trend in L3L than L3W (> 75%), but the overall
 489 range of differences doesn’t shift by much. The L3L – L3W trend difference is significant in 956 of the 2670

490 coastal grid boxes for which the analysis can be performed (36 %), with the range in differences spanning
491 around 4 ppbv y⁻¹. The trends are negative at 75 % of coastal grid boxes in both datasets, this value increasing
492 to 95% when the trend in both L3L and L3W is significant. Descriptive stats corresponding to the trends
493 values compared are detailed in Table 2).

494 To determine whether differences in trend can be linked to differences in retrieval sensitivity, L3L –
495 L3W trend are stratified by L3L – L3W surface level AK rowsum differences (Fig. 5d). As with mean VMR
496 differences, the size of the trend difference tends to increase as the difference in AK rowsums increases. In
497 addition, as the magnitude of AK rowsum difference increases in the positive direction (i.e. increasingly
498 greater sensitivity over land), a greater proportion of trend differences are positive (i.e. a stronger trend over
499 land). This pattern is even more pronounced when restricted to grid boxes where both trends are significant
500 (also shown in Fig. 5d).

501 In summary, these results show a general tendency for trend underestimation in surface level retrievals
502 over water compared to retrievals over land in the same coastal grid boxes obtained at the same times, which
503 appears to be linked to differences in retrieval sensitivity. The relationships found in these analyses are not
504 perfect because trend differences are sensitive to several other factors, in addition to differences in retrieval
505 sensitivity. For example, a greater trend difference would be evident if the rate of change in “true” CO
506 concentrations is faster than if it is slow/negligible, for a given sensitivity difference. Similarly, there should
507 be zero trend difference if “true” CO concentration levels are stable over time, irrespective of the magnitude
508 of difference in retrieval sensitivity. The accuracy of the a priori is a further complicating factor. An
509 underlying assumption is also that the temporal trend in “true” VMRs should not vary much across a 1° x 1°
510 L3 grid box. Hedelius et al. (2021) lends credence to this assumption with the finding that CO trends are
511 similar within regions spanning a few thousand kilometres (L3 grid boxes are ~ 100 km²), and that trends
512 within urban areas are generally indistinguishable from the trend of the broader region encompassing the
513 urban area, despite an expectation that urban trends should exceed the regional background due to a
514 concentration of CO emission sources here.

515
516
517
518
519
520
521

Table 2. Descriptive stats corresponding to the WLS trends detected in L3L, L3W, and L3O_M that are compared in the boxplots of Fig. 5c.

			Mean	Std	Median	IQR
All	L3L – L3W (n = 2670)	L3L	-0.55	1.27	-0.47	1.00
		L3W	-0.49	1.08	-0.34	0.65
	L3L – L3O _M (n = 2670)	L3L	-0.55	1.27	-0.47	1.00
		L3O _M	-0.51	1.03	-0.38	0.73
Both significant (p < 0.1)	L3L – L3W (n = 641)	L3L	-1.39	1.66	-1.15	1.08
		L3W	-1.06	1.56	-0.78	0.92
	L3L – L3O _M (n = 873)	L3L	-1.24	1.64	-1.06	1.07
		L3O _M	-1.02	1.38	-0.83	0.88
Significantly different (p < 0.1)	L3L – L3W (n = 956)	L3L	-0.64	1.39	-0.65	0.92
		L3W	-0.52	1.06	-0.43	0.67
	L3L – L3O _M (n = 555)	L3L	-0.69	1.36	-0.67	0.85
		L3O _M	-0.60	1.00	-0.51	0.68

523

524 3.2.2. Consequences for L3O data with a surface index of mixed (“L3O_M”)

525

526 To recap, L3O data are given the surface index “mixed” when neither land nor water is the dominant surface
 527 type of the bounded L2 retrievals, for a given retrieval time. When this is the case, the retrievals over land
 528 and water are averaged together. Users of L3O data do not have the option of choosing to only analyse the
 529 subset of retrievals made over land (L3L) or water (L3W), as was done in the preceding analysis. To do so
 530 requires the original L2 retrievals. In this section, the L3O_M retrievals are compared to the L3L retrievals that
 531 were analysed in the previous section. The aim here is to demonstrate how, for some L3 grid boxes,
 532 information on “true” VMRs and temporal trends that is available in the L2 retrievals over land (L3L) is
 533 effectively lost to users of L3O data by their averaging together with the less sensitive L2 retrievals over
 534 water (L3W).

535

536

538

539 For long-term mean VMRs, L3O_M unsurprisingly represents a mid-point between L3L and L3W, with lower
540 VMRs than L3L, but a smaller difference range overall than L3W (Fig. 5a, red boxplots). The L3L – L3O_M
541 differences in long-term mean VMR are significant at 45 % (1791) of coastal grid boxes. All but 3 of these
542 grid boxes also see a significant difference between long-term mean VMRs in L3L and L3W. This makes
543 sense: retrievals in L3L would not be expected to differ significantly from those in L3O_M if they do not also
544 differ significantly from L3W. In total, 75 % of grid boxes that feature a significant difference between L3L
545 and L3W also see a corresponding significant difference between L3L and L3O_M. There are several notable
546 differences between this subset of coastal grid boxes (“BOTH”), compared to those that see a significant
547 difference between L3L – L3W but not between L3L and L3O_M (“L3L_L3W_ONLY”), detailed in Table 3a:

548

- 549 • The grid boxes of BOTH see greater retrieved VMR differences between L3L and L3W than the grid
550 box subset of L3L_L3W_ONLY (mean L3L – L3W difference of 13.84 vs 8.67 ppbv). This is logical:
551 L3O_M only differs significantly from L3L if the underlying L3L – L3W difference is sufficiently large
552 to persist through averaging.
- 553 • The grid boxes of BOTH also feature a greater land-water sensitivity contrast than those of
554 L3L_L3W_ONLY. This is indicated both by L3L – L3W AK rowsum differences, driven
555 predominantly by decreased sensitivity over water in BOTH; and by L3L – L3W retrieved minus a
556 priori VMR differences.
- 557 • The grid boxes of BOTH tend to have a greater proportion of their surface covered by water than land
558 when compared to L3L_L3W_ONLY. This is determined by analysis of ratio(land/water) values for
559 each grid box (derivation of this metric is outlined in Sect. 2.4). A mean ratio(land/water) of 0.87 for
560 BOTH indicates a greater water influence on L3O_M than for the grid boxes of L3L_L3W_ONLY, for
561 which a mean ratio(land/water) of 1.00 indicates a more even land/water split. Thus, L3O_M more
562 closely resembles L3W – which is significantly different to L3L – in BOTH than in
563 L3L_L3W_ONLY.

564

565 It is easy to understand how each of these can lead to a L3O_M retrieval that differs significantly from the
566 corresponding L3L retrieval. Interestingly, it is also notable that retrieved and a priori VMRs are lower in
567 BOTH than in L3L_L3W_ONLY, and that retrieved minus a priori VMR values are greater in BOTH than
568 in L3L_L3W_ONLY. This could imply that the a priori VMRs are closer to reality for the grid boxes of

569 L3L_L3W_ONLY than those of BOTH, however further information on “true” VMRs is required to properly
 570 assess this.
 571

Table 3a. Descriptive stats corresponding to matched retrievals over land and water (L3L and L3W) where the long-term mean retrieved surface level VMR in L3L and L3W is significantly different ($p < 0.1$, $n = 2379$). Grid boxes are divided into two subsets depending on whether long-term mean VMRs in L3L and L3O_M are significantly different ($p < 0.1$; “BOTH”) or not ($p > 0.1$; “L3L_L3W_ONLY”). The metric “ratio(land/water)” indicates the relative land vs water surface coverage of a L3 grid box. A ratio(land/water) value > 1 (< 1) implies that more of the grid box surface is covered by land (water).

	BOTH (n = 1788, 75 %)			L3L_L3W_ONLY (n = 591, 25 %)		
Mean ratio(land/water)	0.87			1.00		
	Land	Water	L-W	Land	Water	L-W
Mean vmr_ret	127.21	113.37	13.84	138.30	129.64	8.67
Mean vmr_apr	109.11	108.62	0.49	127.94	126.96	0.98
Mean ret-apr	18.11	4.75	13.36	10.36	2.68	7.68
Mean AK rowsum	0.42	0.16	0.26	0.46	0.26	0.20

572 *Trends in L3O_M*

573
 574 Temporal trends detected in L3O_M are now compared to those in L3L (Fig. 5c, red boxplots). Overall, a
 575 greater number of grid boxes feature a significant trend in both L3L and L3O_M than in L3L and L3W (873
 576 vs 641; 33 % vs 24 %), and fewer see a significant difference between trends (555 vs 956; 21 % vs 36 %).
 577 This is to be expected, given that the L2 retrievals contributing to L3L also contribute to L3O_M. The trends
 578 in L3L and L3O_M are significantly different in just under half (47 %) of the grid boxes where the trend is also
 579 significantly different between L3L and L3W (“BOTH”; Table 3b). These grid boxes are clearly more water-
 580 dominated than the remaining 53 % of grid boxes where the trend difference between L3L and L3W is
 581 significant (“L3L_L3W_ONLY”) but the L3L – L3O_M difference is not. This is indicated by a mean
 582 ratio(land/water) of 0.77 for BOTH vs 0.99 for L3L_L3W_ONLY. Additionally, detected trends in the grid
 583 boxes of BOTH are slightly stronger, with a greater difference between L3L and L3W, than for the
 584 L3L_L3W_ONLY subset. Those L3 grid boxes featuring the strongest land-water trend difference are

585 therefore most likely to also see a significant trend difference between L3L and L3O_M. Again, this is logical.
 586 Unlike with the retrieved VMR comparison above, however, there are no clear differences in mean retrieved
 587 or a priori VMRs, nor sensitivity metrics, between these two grid box subsets (also detailed in Table 3b).
 588 However, it is not necessarily expected that there would be clear differences in these parameters for this
 589 analysis, since trend magnitudes themselves are also a variable (i.e. the trend in “true” CO varies across
 590 space, independent of retrieval sensitivity or CO concentration, complicating the relationships outlined
 591 above).

592 Most of the grid boxes where the L3L and L3O_M trends are significantly different also feature a
 593 significant difference between L3L and L3W (453 of 555; 82 %). There are no clear differences between
 594 these and the remaining 18 % of grid boxes that, counter-intuitively, feature a significant difference between
 595 trends in L3L and L3O_M but not between trends in L3L and L3W. However, small discrepancies are to be
 596 expected for results based on statistical thresholds, especially where the variables being compared are subject
 597 to multiple different factors (e.g. land-water surface cover ratio in L3O_M; land-water sensitivity contrast;
 598 retrieved VMR differences; differences in the “true” CO concentration being retrieved and its change over
 599 time).

Table 3b. Descriptive stats corresponding to matched retrievals over land and water (L3L and L3W) where the temporal trend detected using WLS regression analysis on yearly-mean retrieved surface level VMR in L3L and L3W is significantly different ($p < 0.1$, $n = 956$). Grid boxes are divided into two subsets depending on whether the trend in L3L is significantly different to the corresponding trend detected in L3O_M ($p < 0.1$; “BOTH”) or not ($p > 0.1$; “L3L_L3W_ONLY”). The metric “ratio(land/water)” indicates the relative land vs water surface coverage of a L3 grid box. A ratio(land/water) value > 1 (< 1) implies that more of the grid box surface is covered by land (water).

	BOTH (n = 447, 47 %)			L3L_L3W_ONLY (n = 509, 53 %)		
Mean ratio(land/water)	0.77			0.99		
	Land	Water	L-W	Land	Water	L-W
Mean WLS trend	-0.72	-0.58	-0.14	-0.58	-0.47	-0.11
Mean ABS WLS trend	1.18	0.76	0.42	1.04	0.68	0.35
Mean trend standard error	0.55	0.39	0.16	0.58	0.36	0.22
Mean vmr_ret	128.25	121.36	6.90	129.22	120.20	9.02
Mean vmr_apr	117.21	117.13	0.08	116.01	115.73	0.29
Mean ret-apr	11.05	4.22	6.82	13.21	4.47	8.74
Mean AK rowsum	0.46	0.22	0.25	0.44	0.20	0.24

600

601 3.3. Implications for users of L3O data

602

603 So far, this paper has shown a clear difference in retrieval sensitivity over land and water for coastal grid
604 boxes, demonstrated how long-term VMR statistics and temporal trends calculated using these retrievals
605 (L3L and L3W) differ, and outlined consequences of averaging these retrievals together to create L3O_M. The
606 full time series of available data in L3O is now compared with L3L and L3W, without the constraint that a
607 retrieval needs to be present in both L3L and L3W for it to be included in the analysis. This replicates what
608 a user of the L3O data would do, i.e., work with all available data.

609 Users of MOPITT data are advised to restrict their analysis to retrievals performed over land. This
610 poses a quandary for users of L3O: what to do about days with a surface index of mixed? Therefore, the
611 implications of choosing to include or discard these days are also considered. In the subsequent sections, the
612 following subsets of the full L3O time series for each coastal grid box are analysed: the full L3O time series
613 with no filtering by surface index (“L3O_{NF}”); only days with a surface index of land (“L3O_L”); and days
614 where the surface index is land or mixed (“L3O_{LM}” – i.e., only days with a L3O surface index of water are
615 discarded).

616

617

618 3.3.1. Loss of available data

619

620 The guideline to only analyse retrievals performed over land results in a huge loss of data for coastal grid
621 boxes when using the L3O dataset. We quantify this by comparing the total number of days with data for
622 analysis at each coastal grid box in L3O_L (“n_days(L3O_L)”) and L3O_{NF} (“n_days(L3O_{NF})”) (Fig. 6a).
623 Strikingly, 35 % of coastal grid boxes (total coastal grid boxes = 4299) have zero days in L3O_L, and 67 %
624 have a surface classification of land less than 5 % of the time in L3O (yielding a n_days(L3O_L/L3O_{NF}) ratio
625 of 0.05 or less in Fig. 6a). Importantly, retrievals over land are made on a large proportion of these filtered
626 days; but they are either discarded altogether or averaged together with retrievals made over water to create
627 L3O_M. This point is demonstrated by comparison to the total number of days with data for analysis at coastal
628 grid boxes in L3L (“n_days(L3L)”). In contrast to a mean (median) n_days(L3O_L/L3O_{NF}) ratio of 0.08 (0.01),
629 a mean (median) n_days(L3L/L3O_{NF}) ratio of 0.44 (0.40) demonstrates the stark loss of available data. This
630 is further highlighted by the fact that over half (56%) of coastal grid boxes have at least 25 times more days
631 with retrievals made over land than are available for analysis in the L3O dataset if filtering guidelines are
632 followed (as shown by the ratio n_days(L3L/L3O_L) in Fig. 6b (black line)).

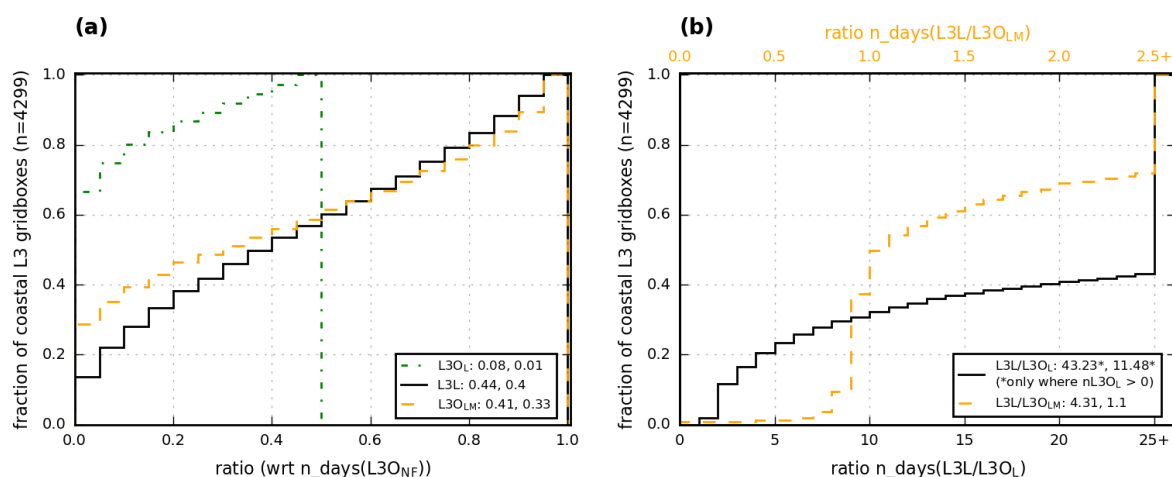


Figure 6. Cumulative frequency histograms comparing the number of days with data for different L3O subsets and L3L at coastal L3 grid boxes. A ratio < 1 (> 1) indicates the plotted dataset has less (more) days with data than the comparison dataset that is indicated on the x-axis. **(a)** L3OL (dash-dot green line), L3L (solid black line), and L3OLM (dashed orange line) are compared to the “as-downloaded” L3O dataset, without any filtering by surface index (“L3ONF”). Values in legend correspond to mean and median ratio for indicated dataset, respectively. Note, as a result of how coastal grid boxes are classified (outlined in Sect. 2.3), all $n_days(L3O/L3ONF)$ ratios are below 0.5 (i.e. at best, L3O has a surface classification of land on 50 % of days) **(b)** L3L is compared with L3OL (solid black line, bottom x-axis) and L3OLM (dashed orange line, top x-axis). Values in legend correspond to mean and median ratios, respectively.

634 The situation can be improved for L3O users by keeping days when the L3O surface index is classified
 635 as mixed, in addition to land (“L3OLM”). Even in this best-case scenario however, L3OLM sees less days with
 636 data than L3L for over 60% of coastal grid boxes ($ratio\ n_days(L3L/L3OLM)$ in Fig. 6b (orange line)).
 637 Moreover, the large proportion of these L3OLM days have the surface index of mixed and therefore suffer
 638 from the averaging together of retrievals over land with retrievals over water which, as has been shown, can
 639 significantly impact the results of analyses using these data. This point is returned to in following sections.

640 Intuitively, it is to be expected that the $ratio\ n_days(L3L/L3OLM)$ should *never* be < 1 . L2 retrievals
 641 over land obviously contribute to days when L3O is classified as land, and should, by definition, also
 642 contribute to days when L3O is classified as mixed. In these cases, L3L will therefore also be present.
 643 However, there are two instances where L2 retrievals over land in fact do not contribute to a L3O retrieval
 644 classified as mixed. Firstly, L2 retrievals themselves also have a classification of mixed, when the L2 retrieval
 645 does not predominantly overlie water or land. L3O can thus have a surface classification of mixed when
 646 created from bounded L2 retrievals that are either only retrieved over a mixed surface, or a combination of

647 mixed and water: in both cases, there are no L2 retrievals over land, and therefore no L3L. Secondly, analyses
648 performed for this paper identified numerous instances where L3O is classified as mixed, but the only
649 contributing L2 retrievals are retrievals over water. In these instances, L3O would therefore seem to be
650 misclassified. On days when this is the case, there will be no corresponding L3L retrieval. This is documented
651 further in the Supp. Mat. (SM6). Attempting to quantify the extent of this misclassification influence is
652 beyond the scope of this paper. In the vast majority of cases where a given grid box has a $n_days(L3L/L3O_{LM})$
653 ratio < 1 , the difference is negligible (i.e. 75 % of these grid boxes have a ratio between 0.9 and 1).
654 Irrespective, in terms of the number of days with retrievals available for analysis, L3L is an improvement
655 over $L3O_{LM}$ for more grid boxes than it is not.

656

657

658 **3.3.2. Scientific implications**

659

660 Long-term mean (ltm) retrieved VMR values from the different L3O subsets are compared to L3L for all
661 coastal grid boxes. As expected from the analyses in Sect. 3.2, all L3O subsets that have some influence from
662 L2 retrievals over water have a ltm retrieved VMR that is below that in L3L, on average (Fig. 7a).
663 Unsurprisingly, the closest match to L3L is $L3O_L$ (mean difference -3.1 ppbv), with the mean difference
664 increasing for each L3O subset as the influence of retrievals over water increases (e.g. $L3O_{LM}$ differs less on
665 average from L3L (mean difference = 5.2 ppbv) than $L3O_{NF}$ (mean difference = 9.1 ppbv), which additionally
666 features days when L3O is solely created from L2 retrievals performed over water).

667 Note that ltm retrieved VMRs in $L3O_L$ and L3L are not a perfect match because $L3O_L$ is only a subset
668 of L3L for each grid box considered in the analysis: L3L may be present on a day when $L3O_L$ is not owing
669 to the way that the L3O data are created (i.e., classified based on the ratio of L2 retrievals over land and
670 water, with retrievals over land potentially being discarded if these are not the majority). Apart from $L3O_L$,
671 less than 25 % of the coastal grid boxes have a retrieved ltm VMR that is greater in an L3O subset than in
672 L3L. The range of ltm differences for each of these L3O subset comparisons to L3L exceeds 35 ppbv
673 (excluding outliers), with over 25 % of coastal grid boxes compared having ltm differences exceeding 9 ppbv
674 (as indicated by boxplot upper quartile values).

675 The percentage of coastal grid boxes that feature a significant difference between ltm retrieved VMRs
676 in L3L and each L3O subset (indicated in blue above each boxplot) is high: strikingly, it is found that, for
677 the two subsets that L3O users could realistically choose to analyse if following data filtering guidelines
678 ($L3O_L$ or $L3O_{LM}$), almost a quarter ($L3O_L$) or almost half ($L3O_{LM}$) of coastal grid boxes see a significant
679 difference to L3L.

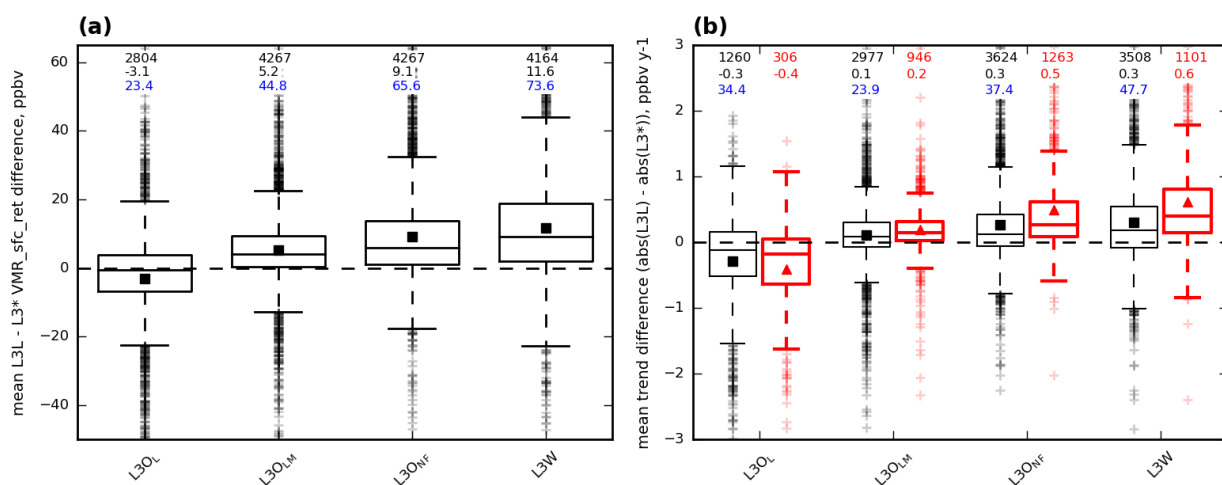


Figure 7. Boxplots showing how mean VMRs and trends compare from selected L3O subsets and L3W to L3L. Values compared are calculated from all available data across the study period. Mean values are represented by filled squares, and values above the boxplots correspond to number of grid boxes with data for that boxplot (black, top row), the mean value (black, second row), and the percentage of grid boxes represented in that boxplot that feature a significant difference with L3L (blue, third row), respectively. The comparison is calculated as $L3L - L3^*$ in both cases; therefore a point above (below) the black $y=0$ line indicates that the value being compared is greater (lower) in L3L. **(a)** Mean VMR differences between L3L and the indicated L3O subset or L3W. Note that the n value is different for each boxplot because not all L3 subsets are present at every coastal grid box, as shown in Sect. 3.3.1. **(b)** Differences in gradients (absolute values) detected using WLS regression analysis between L3L and the indicated L3O subset or L3W. Shown are the differences for all coastal grid boxes where WLS could be performed for both datasets compared (black, mean values represented by filled black squares), and only for the sample of those grid boxes where the detected trend is significant ($p < 0.1$) in both (red, thicker lines, mean values represented by filled triangles).

681 The results of WLS regression analysis on yearly mean values from each dataset are now compared.
 682 As expected from the earlier analysis, trends are strongest, on average, in L3L and L3O_L – this is especially
 683 so when the comparison is restricted only to trends that are significantly different from zero ($p < 0.1$) (Table
 684 4). These datasets also have the largest measures of spread, indicating their tendency to yield stronger trends
 685 than the other L3O subsets (and L3W), and these measures lessen for each L3O subset as the influence of
 686 retrievals over water increases. Concomitant with trends decreasing in strength as the influence of retrievals
 687 over water increases in each L3O subset, overall retrieval sensitivity also decreases, as indicated by the mean
 688 averaging kernel metrics shown in Table 4. Comparing the magnitude of trends at each coastal grid box,
 689 significant trends are stronger in L3L for at least 75% of grid boxes for all comparison datasets apart from
 690 L3O_L (Fig. 7b). L3O_L sees stronger trends than L3L on average, but the comparison of these two datasets
 691 needs to be interpreted with caution due to L3O_L being a subset of L3L that features far fewer days with data,

692 as discussed previously. Like with ltm retrieved VMRs discussed above, the percentage of coastal grid boxes
 693 that feature a significant difference between trends detected in L3L and each L3O subset is high, with over a
 694 third (almost a quarter) of the trends in L3O_L (L3O_{LM}) being significantly different to L3L.
 695
 696

Table 4. Descriptive stats corresponding to the WLS trends detected in L3L, L3W, and selected L3O subsets. Also shown are mean averaging kernel rowsums and diagonal values corresponding to the retrievals from which trends are calculated.

		L3L	L3O _L	L3O _{LM}	L3O _{NF}	L3W
Calculated from all gridboxes where WLS could be performed	Number of grid boxes	3624	1260	2999	4288	4169
	Mean (std) trend	-0.59 (1.22)	-0.52 (1.38)	-0.50 (0.95)	-0.54 (0.67)	-0.54 (0.66)
	Median (IQR) trend	-0.45 (0.89)	-0.46 (1.08)	-0.37 (0.67)	-0.42 (0.53)	-0.40 (0.54)
	Mean AK rowsum	0.45	0.45	0.33	0.28	0.22
	Mean AK diagonal value	0.10	0.10	0.08	0.07	0.06
Calculated only from gridboxes where WLS trend is significant (p < 0.1)	Number of grid boxes	1447	453	1265	2588	2499
	Mean (std) trend	-1.23 (1.55)	-1.17 (1.90)	-0.95 (1.18)	-0.79 (0.73)	-0.78 (0.72)
	Median (IQR) trend	-0.98 (0.94)	-1.09 (1.28)	-0.74 (0.75)	-0.62 (0.56)	-0.62 (0.57)
	Mean AK rowsum	0.51	0.48	0.39	0.33	0.29
	Mean AK diagonal value	0.11	0.10	0.08	0.07	0.06

697
 698
 699
 700
 701
 702
 703
 704
 705
 706
 707
 708
 709

3.4. Illustrative examples comparing L3O and L3L: analysis of the most populous coastal cities

In this section, we analyse time series from the 33 L3 coastal grid boxes that contain cities classified amongst the 100 most populous in the world (derivation outlined in Sect. 2.5) to illustrate the differences between mean values and trends obtained from the L3O and L3L datasets. We focus our comparison on L3O_L and L3O_{LM}, as these are the L3O subsets that data users would realistically choose to analyse if following the data filtering guidelines. For clarity, from here these grid boxes are referred to by the name of the city that they contain. A detailed case study for the L3 grid box containing the city of Dubai is first presented, before considering results for all cities analysed.

3.4.1. Detailed case study: L3 grid box containing Dubai

Summary stats derived from the L3O subsets, L3L, and L3W (included for comparison), for the L3 grid box containing the city of Dubai, are given in Table 5. Figure 8 visualises the daily retrieved VMR time series from L3L, with L3O_L overlaid for comparison purposes.

Of a possible 1620 days with data in the unfiltered L3O dataset for this grid box, a mere 70 days (4 %) remain for analysis when following data filtering guidelines to restricting analysis to retrievals performed over land only (the L3O_L subset). By contrast, there are 1523 days available for analysis using the L3L dataset for this grid box (94 % of total days with retrievals in the L3O dataset). However, in L3O, on most days these retrievals over land are averaged together with retrievals over water to create L3O_M, as evidenced by the L3O_{LM} subset containing 1486 days with data for this grid box (92 % of total days in the L3O dataset). That L3L has a greater number of days with data than the L3O_{LM} subset indicates that there are days in L3O with a surface index of water where L2 retrievals were present over land but were discarded because of the L3 creation process.

Long-term mean retrieved VMR is greatest in the land-only datasets L3O_L and L3L. The value in L3O_L is 10 ppbv greater than in L3L. Given that L3O_L is a very small subset of L3L, this appears to be a large overestimate, when compared to L3L. Long-term mean retrieved VMR in L3O_{LM} is 11 ppbv lower than in L3L. This is clearly a result of the inclusion of retrievals over water in this dataset, via L3O_M, with long-term mean retrieved VMR in L3W being 17 ppbv lower than L3L. Both the L3L vs L3O_{LM} and L3L vs L3W mean differences are significant ($p < 0.1$). Consistent with the results shown in Sect. 3.2.2 when identifying factors that determine whether the averaging of L2 retrievals over land and water to create L3O_M can yield statistically significantly different retrievals to L3L, this L3 grid box is water-dominated, with a mean ratio(land/water) of 0.60.

The trends detected using WLS analysis following the method outlined in Section 2.5 are visualised in Figure 9 (note that trend values are also given in Table 5 in both ppbv y^{-1} and $\% \text{ y}^{-1}$), along with the yearly mean VMR values that were used in the regression. Detected trends are clearly strongest in the land-only datasets L3O_L and L3L, with the L3O_L trend being significantly stronger ($p < 0.1$) than the L3L trend – a difference of equating almost $1 \% \text{ y}^{-1}$ (2.01 ppbv y^{-1}). Again, given the far superior temporal coverage of L3L, this is the more reliable result. The trend in L3L is $0.65 \% \text{ y}^{-1}$ (1.28 ppbv y^{-1}) stronger than in L3O_{LM}, which corresponds to a difference of almost 12 % over the 18-year period of analysis. The trend in L3O_{LM} is clearly weakened by inclusion of retrievals over water, with the trend in L3W being over $1 \% \text{ y}^{-1}$ weaker than in L3L. Note that this trend analysis has been repeated using an alternative regression method which is less

Table 5. Summary stats from L3O subsets compared, L3L, and L3W (for comparison), for the L3 grid box containing the city of Dubai. Note that across the whole study period (2001-09-01 to 2018-12-31), there are 5988 MOPITT files available. There are 1620 days with data in the L3O dataset (unfiltered by surface index), 27 % of the whole study period. The WLS trend in units of $\% y^{-1}$ is calculated by dividing the trend in units of $ppbv y^{-1}$ by the respective long-term mean VMR value.

Dataset	n days with data (% of days in L3O (n = 1620))	Long-term mean VMR (\pm standard deviation) (ppbv)	WLS trend (\pm standard error) (ppbv y^{-1})	WLS trend (\pm standard error) (% y^{-1})
L3O _L	70 (4 %)	190 (\pm 56)	-4.91 (\pm 1.21)	-2.59 (\pm 0.64)
L3O _{LM}	1486 (92 %)	169 (\pm 25)	-1.62 (\pm 0.18)	-0.96 (\pm 0.10)
L3L	1523 (94 %)	180 (\pm 44)	-2.90 (\pm 0.26)	-1.61 (\pm 0.14)
L3W	1565 (97 %)	163 (\pm 18)	-0.90 (\pm 0.13)	-0.55 (\pm 0.08)

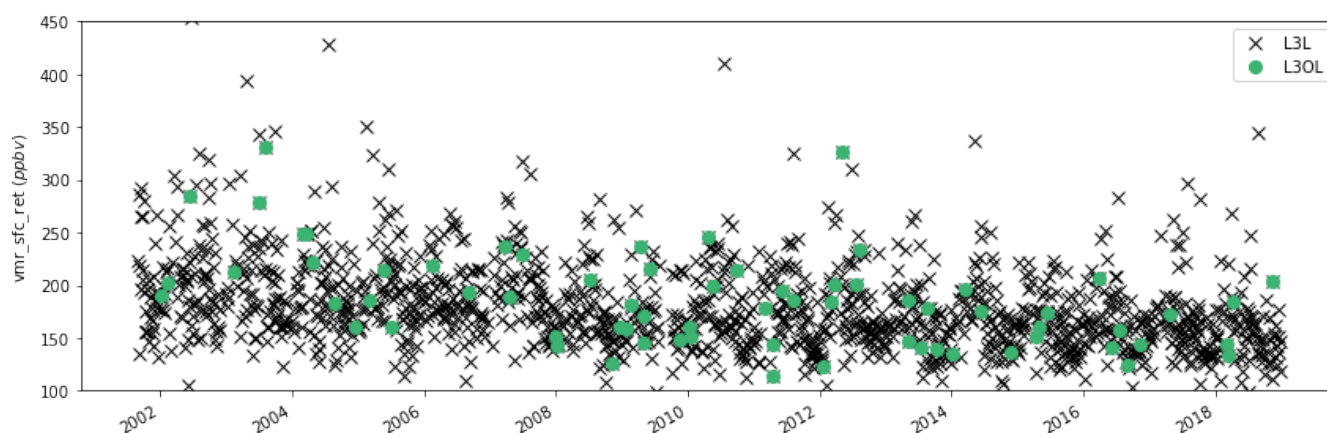


Figure 8. L3L (black crosses) and L3O_L (green circles) time series for the entire study period. Note that the size of plotted symbol required to visualise the whole time series artificially exaggerates the sense of temporal coverage; in reality, L3L is only present on 25 % of the days across the study period, and L3O_L just 1 %.

744 sensitive to outlying values (Theil-Sen slope estimator), and the results are unchanged. This is detailed further
745 in the Supp. Mat. (SM7).

746 To summarise: If L3O users follow data filtering guidelines and restrict analysis to retrievals only
747 performed over land, there is a huge loss of data coverage in the L3O dataset for the coastal L3 grid box
748 containing the city of Dubai. Choosing to work with L3O_L despite this would lead to results that are clearly
749 erroneous, when compared to L3L, which has far greater temporal coverage (almost 22 times more days with

750 data than L3O_L). L3O users could make the decision to include days with a L3 surface classification of
 751 “mixed” into their analysis to increase temporal coverage (the L3O_{LM} dataset analysed here). However, doing
 752 so would yield both lower retrieved VMRs, on average, and significantly weaker decreasing trends, than
 753 L3L. This is demonstrably due to the incorporation of retrievals over water into L3O_{LM} (via L3O_M), as shown
 754 by the comparison with L3W.
 755

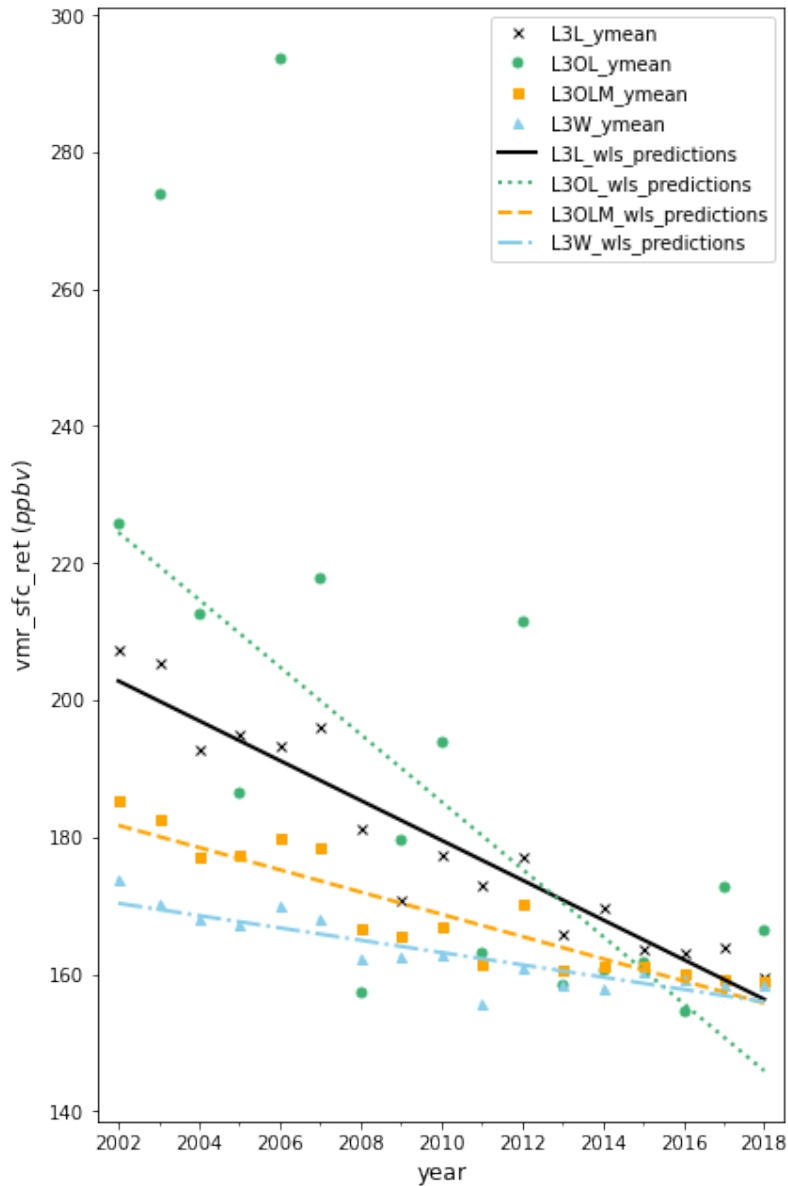


Figure 9. Yearly mean retrieved VMR in the different datasets being investigated, and the trendlines obtained from WLS regression analyses on each of these datasets. Black crosses and solid black lines correspond to L3L; green filled circles and dotted green lines correspond to L3O_L; orange filled squares and dashed orange lines correspond to L3O_{LM}; blue filled triangles and dash-dot blue lines correspond to L3W. Trend values for each dataset are also given in Table 5.

756

757 3.4.2. Discussion of results for all cities analysed

758

759

760 The above analysis is repeated for all cities of interest. Number of days with data, long-term mean retrieved
761 VMRs, and temporal trends are given in Table 6 for the L3 grid boxes containing these cities for each of the
762 L3O subsets considered, L3L, and L3W (for comparison). These metrics are evaluated in turn below.

763

764 *Temporal coverage*

765

766 The loss of data in L3O if filtering for retrievals over land only (L3O_L) is clear: 6 of the cities cannot be
767 studied at all using L3O_L (number of days with data = 0), and of the remaining 27 cities with data in this L3O
768 subset, only a single city (Osaka) has more than 50 % of the days with data in L3L. The mean
769 $n_days(L3O_L/L3L)$ ratio for these 27 cities is 0.18 – i.e., on average, there are over 5 times more days with
770 data in L3L than are available in L3O when filtering for retrievals over land only.

771 L3O_{LM} compares more favourably to L3L in terms of number of days with data, due to the inclusion
772 of days when the L3O surface index is “mixed”, with a mean $n_days(L3O_{LM}/L3L)$ ratio of 0.85.
773 $n_days(L3O_{LM}) > n_days(L3L)$ for 11 of the 33 cities, although the difference is generally small. L3O_M is
774 the dominant component of L3O_{LM} in all cases here, being the classification on 84 % of days, on average,
775 across all 33 cities (max = 100 %, min = 45 %).

776

777 *VMR comparison*

778

779 The consequence of the loss of data in L3O_L is clear: compared to L3L, mean VMR in L3O_L is higher, and
780 the magnitude of this difference generally depends upon how much data is lost in L3O_L. Mean VMR across
781 all cities (excluding the 6 cities where $n_days(L3O_L) = 0$) is 17 ppbv higher in L3O_L than in L3L. This falls
782 to 10 ppbv if restricted to cities where the $n_days(L3O_L/L3L)$ ratio is greater than 0.05 (n=17), and 7 ppbv if
783 restricted to cities where the $n_days(L3O_L/L3L)$ ratio is above 0.2 (n=11). The mean VMR difference (L3L
784 – L3O_L) is significant ($p < 0.1$) for 11 of the 27 cities that can be compared; in these cases, L3O_L is a smaller
785 subset of L3L than for the cities where mean VMR difference is not significant ($n_days(L3O_L/L3L) = 0.15$
786 vs 0.22, respectively), and the mean VMR difference is unsurprisingly much greater (-36 vs -4 ppbv).

787

788

Table 6. Summary stats for the L3 grid boxes containing the 33 cities of interest from each of the L3O subsets considered, L3L, and L3W (for comparison). For each grid box and dataset, the following stats are shown: 1. ratio(land/water), which is an indicator of the relative land vs water surface coverage of a L3 grid box; 2. the number of days with data across the whole study period; 3. the mean retrieved VMR (\pm the standard deviation), in ppbv; and 4. the trend from WLS regression analysis (\pm the standard error), in ppbv y^{-1} . Dash symbols ('-') indicate that the stat cannot be calculated for a given grid box and dataset owing to lack of data. Yellow shading indicates that a dataset mean or trend value is significantly different to the value in L3L for that city ($p < 0.1$). Grey shading indicates that the trend value is not significantly different to zero ($p < 0.1$). Diagonally striped yellow-grey shading indicates that the trend value is not significantly different to zero AND that it is significantly different to the trend in L3L for that city.

¹ The modified mean, shown in the bottom row of the table, corresponds to the mean value that is calculated only for cities where there is a corresponding stat in the L3O_L dataset. For 1-3, this corresponds only to cities where number of days with data L3O_L > 0 (n = 27). For 4, this corresponds only to cities where there are enough days with data for the regression analysis to be performed in L3O_L (n = 18). By contrast, the mean value, shown in the penultimate table row, simply represents the mean of all values in that column

city	1. ratio (land/water)	2. number of days with data				3. mean (\pm std) [ppbv]				4. trend (\pm standard error) [ppbv y ⁻¹]			
		L3L	L3O _L	L3O _{LM}	L3W	L3L	L3O _L	L3O _{LM}	L3W	L3L	L3O _L	L3O _{LM}	L3W
Tokyo	1.57	620	98	627	575	185 (43)	188 (38)	184 (36)	178 (34)	-1.7 (0.3)	-2.3 (0.5)	-1.7 (0.3)	-1.7 (0.3)
Shanghai	1.35	378	54	374	416	373 (130)	374 (112)	363 (111)	338 (108)	-5.9 (1.4)	-7.0 (1.6)	-5.7 (1.4)	-3.4 (1.2)
Manila	0.05	127	0	86	811	150 (28)	-	151 (19)	145 (22)	-1.3 (0.5)	-	-1.2 (0.4)	-1.3 (0.2)
Mumbai	0.12	790	1	388	1356	227 (166)	291 (0)	218 (56)	184 (66)	-1.2 (0.9)	-	-0.6 (0.6)	-0.1 (0.3)
New York	0.07	216	0	178	919	296 (69)	-	315 (59)	332 (64)	-1.4 (1.1)	-	-2.3 (0.8)	-1.9 (0.5)
Lagos	0.13	116	4	92	660	337 (109)	312 (75)	305 (67)	232 (69)	1.2 (2.0)	-	0.5 (1.7)	0.2 (0.4)
Bangkok	0.52	445	33	415	755	314 (77)	346 (78)	308 (62)	261 (79)	-3.0 (0.6)	-8.6 (2.1)	-3.1 (0.7)	-2.0 (0.4)
Osaka	2.08	297	171	309	270	187 (48)	189 (39)	183 (39)	172 (34)	-2.5 (0.5)	-2.3 (0.5)	-2.3 (0.4)	-1.3 (0.4)
Karachi	1.83	1108	423	1117	884	139 (33)	130 (32)	136 (30)	131 (30)	-0.8 (0.2)	-0.6 (0.2)	-0.7 (0.2)	-0.5 (0.3)
Buenos Aires	3.05	864	241	863	719	94 (18)	95 (17)	94 (16)	95 (16)	-0.1 (0.1)	-0.5 (0.2)	-0.2 (0.1)	-0.1 (0.1)
Istanbul	0.11	322	2	436	998	152 (30)	185 (25)	154 (19)	157 (21)	-1.2 (0.4)	-	-0.4 (0.2)	-0.8 (0.2)
Chennai	0.08	331	0	95	1133	223 (56)	-	205 (25)	203 (28)	0.0 (0.8)	-	0.5 (0.5)	-0.9 (0.3)
Xiamen	0.08	215	1	97	854	263 (74)	402 (0)	258 (69)	232 (67)	-2.6 (0.9)	-	-4.1 (1.7)	-1.9 (0.4)
Taipei	0.01	36	0	5	758	192 (50)	-	210 (26)	183 (43)	-3.7 (1.0)	-	-	-1.5 (0.4)
Kuala Lumpur	0.95	142	60	143	200	233 (81)	239 (109)	234 (84)	238 (97)	-2.7 (1.3)	-3.4 (1.2)	-3.9 (1.0)	-5.1 (1.1)
Saigon	1.50	249	122	255	325	254 (65)	267 (62)	244 (60)	189 (51)	-1.4 (0.9)	-3.6 (1.3)	-2.3 (0.8)	-2.3 (0.8)
Luanda	0.67	173	54	175	341	260 (101)	312 (100)	268 (101)	213 (109)	-0.5 (2.1)	-2.6 (3.7)	0.5 (2.2)	-0.2 (1.0)
San Francisco	0.23	522	15	598	889	236 (92)	237 (67)	243 (53)	250 (60)	-1.1 (0.7)	-	-0.7 (0.5)	-1.0 (0.6)
Singapore	0.05	32	0	18	425	387 (248)	-	387 (117)	341 (133)	-	-	-	-4.3 (2.4)
Shantou	1.79	396	175	398	457	312 (96)	326 (104)	304 (91)	264 (80)	-5.4 (0.5)	-5.9 (1.4)	-5.7 (0.4)	-3.8 (0.7)
Hong Kong	0.14	228	3	164	704	336 (83)	432 (70)	312 (71)	260 (93)	-8.1 (0.9)	-	-5.1 (1.3)	-3.5 (0.5)
Toronto	2.85	401	186	416	274	238 (58)	232 (50)	239 (47)	254 (44)	-1.1 (0.8)	-0.3 (1.1)	-1.2 (0.7)	-2.0 (0.6)
Miami	0.35	411	32	357	1038	161 (32)	157 (26)	160 (25)	143 (25)	-1.5 (0.4)	-1.2 (1.2)	-1.3 (0.3)	-0.8 (0.2)
Surat	1.68	943	289	940	760	181 (44)	175 (43)	182 (43)	179 (54)	-0.4 (0.3)	-1.6 (0.7)	-0.4 (0.3)	-0.1 (0.3)
Dar Es Salaam	0.01	44	0	17	1040	103 (46)	-	86 (12)	86 (17)	-0.3 (0.7)	-	-	-0.2 (0.1)
Qingdao	2.35	587	186	589	566	372 (102)	365 (96)	370 (94)	383 (111)	-3.8 (1.5)	-2.0 (1.7)	-3.7 (1.4)	-4.2 (0.9)
Yangon	0.41	590	6	498	930	271 (70)	236 (37)	281 (66)	266 (79)	-1.5 (0.8)	-	-1.7 (0.6)	-2.1 (0.5)
Abidjan	0.48	86	38	83	349	218 (58)	232 (59)	215 (58)	156 (44)	-2.1 (1.4)	-3.6 (1.8)	-0.3 (1.4)	-0.7 (0.3)
Wenzhou	0.56	386	25	347	705	268 (75)	308 (122)	256 (65)	231 (64)	-4.2 (0.7)	-10.1 (2.4)	-3.5 (0.6)	-2.8 (0.6)
Sydney	0.38	709	6	676	1000	94 (36)	92 (17)	90 (16)	87 (15)	-0.7 (0.2)	-	-0.5 (0.1)	-0.2 (0.1)
Accra	0.17	155	7	116	740	245 (84)	262 (68)	224 (63)	161 (48)	2.9 (1.5)	-	2.9 (0.8)	-0.5 (0.3)
Dubai	0.60	1523	70	1486	1565	180 (44)	190 (56)	169 (25)	163 (18)	-2.9 (0.3)	-5.0 (1.2)	-1.6 (0.2)	-0.9 (0.1)
Chittagong	0.81	653	49	628	888	296 (66)	316 (79)	304 (66)	296 (91)	-0.7 (0.5)	-2.1 (2.2)	-0.7 (0.5)	-0.9 (0.7)
Mean	0.82	427	71	394	736	236	255	232	212	-1.9	-3.5	-1.7	-1.6
Modified mean ¹	0.99	493	87	466	712	238	255	233	212	-2.3	-3.5	-2.1	-1.8

790
791
792
793
794
795
796
797
798
799
800
801
802
803
804
805
806
807
808
809
810
811
812
813
814
815
816
817
818
819
820
821
822

The L3L – L3O_{LM} mean VMR difference is relatively small, by comparison (4 ppbv, all 33 cities). However, this does hide some much larger discrepancies between L3L and L3O_{LM} for certain cities, with the difference exceeding 10 ppbv in 11 cases and 20 ppbv for 3 of them. The difference is significant ($p < 0.1$; “SIGDIFF”) for 13 of 33 cities (39 %). Compared to the subset where the L3L – L3O_{LM} mean difference is not significant ($n = 20$, 61 %; “NOT_SIGDIFF”), the following characteristic differences are found (also detailed in Table 7):

- The grid boxes in SIGDIFF have a greater proportion of their surface covered by water than NOT_SIGDIFF: this is evidenced by a mean ratio(land/water) of 0.51 in SIGDIFF vs 1.02 in NOT_SIGDIFF, indicating there are relatively more retrievals over water than land in the former; and also by the fact that on average, L3O_L only contributes to L3O_{LM} in SIGDIFF on 9 % of days, vs 20 % of days for NOT_SIGDIFF (which means that retrievals over water contribute via L3O_M more frequently to L3O_{LM} in SIGDIFF than NOT_SIGDIFF).
- The L3L – L3W VMR_RET differences are larger in SIGDIFF than NOT_SIGDIFF (mean = 31.15 vs 18.44 ppbv), meaning they are less likely to be hidden by averaging to create L3O_M.
- Land-water mean averaging kernel differences suggest there is not a large land-water sensitivity contrast between the SIGDIFF and NOT_SIGDIFF subsets. However, the L3L – L3W ret-apr difference, which is another indicator of sensitivity difference, is much greater for SIGDIFF than NOT_SIGDIFF(21.66 vs 3.22 ppbv, respectively (21.98 vs 11.88 ppbv if using absolute values)). There is some evidence that this may be a function of the a priori VMRs being closer to “true” VMRs in NOT_SIGDIFF, with mean retrieved minus a priori VMR values being closer to zero than in SIGDIFF.

These findings are all consistent with what was shown in Sect. 3.2.2 when identifying factors that determine whether the averaging of L2 retrievals over land and water to create L3O_M can yield a statistically significantly different retrieval to L3L. As outlined above, L3O_M is the dominant component of L3O_{LM} in all cases considered here (being the classification on 84 % of days, on average (max = 100 %, min = 45 %)).

Table 7. Selected parameters from L3 grid boxes containing cities, stratified according to whether mean VMR in L3L and L3O_{LM} is significantly different (“SIGDIFF”; $p < 0.1$) or not (“NOT_SIGDIFF”).

	P < 0.1 (“SIGDIFF”) (n = 13)	P > 0.1 (“NOT_SIGDIFF”) (n = 20)
Mean ratio(land/water)	0.51	1.02
% days from L3O _L	9	20
Δ VMR_RET (L3L – L3W) (ppbv)	31.15	18.44
Δ AK rowsum (L3L – L3W)	0.25	0.21
Δ AK diagonal (L3L – L3W)	0.10	0.08
Δ VMR (RET - APR) (L3L – L3W) (ppbv)	21.66	3.22
Δ VMR (RET - APR) (L3L – L3W) (ppbv)	21.98	11.88
L3L VMR (RET - APR)	-19.82	-7.07
L3L VMR (RET - APR)	39.86	18.79
L3W VMR (RET - APR)	-14.75	-6.73
L3W VMR (RET - APR)	18.21	15.57

824

825

826 *Trend comparison*

827

828 On average, the strongest trends are seen in L3O_L. However, as with the Dubai case study, this often appears
 829 as an outlier compared to the other datasets – a consequence of its comparatively very sparse temporal
 830 coverage. As expected from previous sections, the weakest trends are detected in L3W, with L3O_{LM}
 831 representing a mid-point between this and L3L.

832 Of the 18 cities where WLS analysis can be performed in L3O_L, there are 9 where the resulting trend
 833 – and thus conclusion drawn from the analysis – is significantly different to that in L3L. In 3 of these cases
 834 (Dubai, Wenzhou, Bangkok), the trend in L3O_L can be judged to be a strong over-estimate given the large
 835 difference to the corresponding trends in L3L (trend standard errors do not overlap), and the very small
 836 number of days with data that these trends are based on when compared to L3L ($n_days(L3O_L/L3L)$ ratio <
 837 0.08 in each case). There are 4 additional cities where a significant trend in L3O_L appears to be an over-
 838 estimate, when compared the L3L: Abidjan, Surat, Saigon, and Buenos Aires. This is because the trend for
 839 these cities in L3L is not significantly different to 0 which, given the higher number of days with data in L3L
 840 ($n_days(L3O_L/L3L)$ ratio = 0.44, 0.31, 0.49, 0.28, respectively), appears to be the more reliable result. The

841 L3O_L trend for Miami is insignificant and derived from very low n. L3O_L is also the only dataset to yield an
842 insignificant trend for Qingdao.

843 As with mean VMRs, trends in L3O_{LM} compare better than L3O_L to L3L. However, there are still 5
844 cases where L3O_{LM} and L3L yield significantly different results. For 3 of these (Hong Kong, Istanbul, and
845 Dubai, as covered in detail in Sect. 3.4.1), interpretation of the difference is simple: L3O_{LM} is a significant
846 under-estimate of the CO change over time. This is very likely due to the inclusion of retrievals over water
847 in this dataset, as evidenced by L3W yielding a significantly weaker trend than L3L in all 3 cases. In the
848 remaining 2 cases – New York and Saigon – interpretation is more complicated. For both these cities, the
849 trend detected in L3L is not significantly different from zero, whereas the trend in L3O_{LM} is. Does this mean
850 that the trend in L3O_{LM} is an over-estimate? Possibly. However, in both cases, the trends are within one
851 standard error of each other and therefore within the range of sampling uncertainty. There are an additional 2
852 cities where WLS could be performed in L3L but not L3O_{LM} (Dar Es Salaam and Taipei), but n_{days}(L3L)
853 is so low (44 and 36, respectively) that these results are not deemed to be trustworthy.

854 As outlined in Sect. 2.5, it is important to note that the trends presented in this section are for
855 illustratory purposes only, with the intention of demonstrating that different results can be obtained depending
856 on whether L3O or L3L (and, by extension, L2) data are analysed. More focused analysis is needed to verify
857 these trends, which is beyond the scope of this paper. The trend analysis has been repeated using an alternative
858 regression method which is less sensitive to outlying values (Theil-Sen slope estimator), and the main results
859 reported above stand. This is detailed further in the Supp. Mat. (SM7).

860
861

862 **4. Summary and Conclusions**

863

864 Motivated by the work of Ashpole and Wiacek (2020) which demonstrated, for the MOPITT L3 grid box
865 containing the coastal city of Halifax, Canada, that mean VMR statistics and temporal trends differ depending
866 on whether L2 or L3 data are analysed, this paper has examined what proportion of all coastal L3 grid boxes
867 also see differences between results from analyses performed with L2 and L3 data. While it is recommended
868 to MOPITT data users that analyses are restricted to retrievals performed over land owing to known
869 sensitivity issues over water (MOPITT Algorithm Development Team, 2018; Deeter et al., 2015), such
870 recommendations cannot practically be followed by users of L3 data for coastal grid boxes owing to the way
871 the data are created from their bounded L2 retrievals. In short, this study has sought to answer the question:
872 “does it matter”? Analysis has focussed on comparing the original, “as-downloaded” L3 dataset (“L3O”)

873 with new land-only and water-only L3 products (“L3L” and “L3W” respectively) that have been created from
874 the L2 retrievals. The main results are summarised below.

875 First, a direct comparison of the L2 retrievals performed over land (L3L) and water (L3W) that are
876 averaged together to create L3 products on days when the L3 surface index is “mixed” (L3O_M) identified
877 that:

- 878
- 879 • Retrieval information content is clearly greater in L3L than L3W. The corresponding mean L3L –
880 L3W VMR difference is over 10 ppbv, significant ($p < 0.1$) at 60 % of the coastal grid boxes
881 compared.
- 882 • Temporal trends are also stronger, on average, in L3L (mean diff = 0.28 ppbv y^{-1} , 0.43 ppbv y^{-1} if
883 only considering trends significantly different to zero), with the L3L – L3W trend difference
884 significant ($p < 0.1$) at 36 % of grid boxes where a trend comparison was possible.
- 885 • Larger L3L – L3W differences in mean VMRs and trends are clearly associated with greater
886 differences in retrieval sensitivity.
- 887 • The resulting VMRs in L3O_M are significantly different to L3L for 75 % of grid boxes where the
888 L3L – L3W difference is also significant; this corresponds to 45 % of all coastal grid boxes
889 compared. Whether or not L3O_M and L3L differ significantly depends on multiple factors including
890 the ratio of land/water surface cover in the grid box, the strength of the land-water sensitivity contrast
891 and VMR difference, and, potentially, the accuracy of the a priori.
- 892 • Just under half of the grid boxes that featured a significant L3L – L3W trend difference also see
893 trends differing significantly between L3L and L3O_M. As with the mean VMR comparison, these
894 grid boxes are more water-dominated than the subset whereby the L3L – L3W trend difference is
895 significant but the L3L – L3O_M trend difference is not. They also feature stronger L3L – L3W trend
896 differences overall, but no other variables (such as ltm VMRs and sensitivity metrics) show clear
897 differences.

898

899 Having established the degree of difference in L3O_M and L3L retrievals that is caused directly by
900 averaging L3L with the less-sensitive L3W, the full L3O dataset with differing surface filtering options was
901 compared to L3L:

- 902
- 903 • If L3O is filtered so that only retrievals over land (L3O_L) are analysed, as has been recommended
904 (MOPITT Algorithm Development Team, 2018; Deeter et al., 2015), there is a huge loss of data, in
905 terms of days with data to analyse. This is a direct result of L2 retrievals over land routinely being

906 discarded during the L3O creation process, or averaged with L2 retrievals over water, creating L3O_M
907 (at least for coastal grid boxes). The problem can be alleviated by also retaining L3O_M retrievals, but
908 these additional days with data feature some influence from retrievals made over water that can affect
909 results, as outlined. The resulting L3O_{LM} subset still has less days with data than in L3L for 61 % of
910 coastal grid boxes.

- 911 • Almost a quarter (half) of coastal grid boxes see a significant difference in ltm VMR between L3L
912 and L3O_L (L3O_{LM}). Over a third (almost a quarter) of the trends in L3O_L (L3O_{LM}) are significantly
913 different to L3L.
- 914 • Focusing on the L3 grid boxes containing the 33 largest coastal cities in the world, mean VMRs in
915 L3O_L and L3L differ significantly for 11 of the 27 grid boxes that can be compared (40 %; there are
916 no L3O_L data for the remaining 6 cities). The L3L – L3O_{LM} mean VMR difference across all 33 grid
917 boxes is relatively small (3.7 ppbv), but this does hide some much larger discrepancies, with the
918 difference exceeding 10 ppbv for 11 of the 33 grid boxes and 20 ppbv for 3 of them. The difference
919 is significant for 13 of 33 grid boxes (39 %). Of the 18 grid boxes where WLS analysis can be
920 performed in L3O_L, there are 9 cases where the trend is significantly different to that in L3L. The
921 trends in L3O_{LM} and L3L differ significantly for 5 of the 33 grid boxes.

922
923 From these results, it can be concluded that, yes, for at least a quarter of all MOPITT coastal L3 grid
924 boxes, it does matter that there is limited capacity to filter out the influence of retrievals over water in L3
925 data – at least without a huge loss of temporal coverage. Demonstrably, there are significant differences in
926 the mean VMRs and temporal trends that can be obtained using L3O and L3L, sometimes very large. These
927 differences could have tangible consequences, depending on the purpose for which the MOPITT data are
928 being used. While acknowledging that this analysis has also shown that there is a sizeable proportion of
929 coastal grid boxes where statistically, mean VMRs and trends do not differ significantly between L3L and
930 L3O, there is enough evidence to support the suggestion from Ashpole and Wiacek (2020) that an additional
931 L3 “land-only” product, created only from averaging bounded L2 retrievals performed over land – the L3L
932 dataset that has been analysed in this paper – could be beneficial to the research community. This dataset
933 enables L3 users to maximize retrieval information content for coastal L3 grid boxes, as is currently only
934 possible with L2 data, while also preserving the benefits of L3 products, such as smaller file size and greater
935 accessibility of gridded products. The L3L dataset analysed in this paper is publicly available for download
936 (Ashpole and Wiacek, 2022; L3W is also available). Although this paper has focused only on analysis of
937 MOPITT data, it is reasonable to question whether the findings are applicable to data products from other
938 satellite instruments that make CO retrievals based on observed thermal-infrared radiances, such as AIRS

939 (Atmospheric InfraRed Sounder), TES (Tropospheric Emission Spectrometer), and IASI (Infrared
940 Atmospheric Sounding Interferometer).

941

942

943

944

945 **Data availability**

946

947 The “L3L” and “L3W” datasets analysed in this study are available from the following link:
948 <https://doi.org/10.5683/SP3/ERCG2H> (see also Ashpole and Wiacek, 2022). Code for creating these datasets
949 is available here: https://github.com/ianashpole/MOPITT_L3L_L3W. The MOPITT V8 joint TIR-NIR files
950 Level 2 (“MOP02J”) and Level 3 (“MOP03J”) datasets can be accessed from the following URLs,
951 respectively: https://doi.org/10.5067/TERRA/MOPITT/MOP02J_L2.008 (NASA/LARC/SD/ASDC, 2000a)
952 and https://doi.org/10.5067/TERRA/MOPITT/MOP03J_L3.008 (NASA/LARC/SD/ASDC, 2000b)

953

954

955 **Author contributions**

956

957 IA and AW jointly conceived of and designed the study. IA performed data analysis; both authors examined
958 and interpreted the results, and prepared the manuscript.

959

960

961 **Competing interests**

962

963 The authors declare that they have no conflict of interest.

964

965

966 **Acknowledgements**

967

968 The authors received funding from the Canadian Space Agency through the Earth System Science Data
969 Analyses program (grant no. 16SUASMPTN), the Canadian National Science and Engineering Research
970 Council through the Discovery Grants Program, and Saint Mary’s University. We thank the MOPITT team

971 for providing the data used in this study. The authors would also like to thank two anonymous reviewers and
972 the associate editor whose thoughtful comments helped to improve this manuscript.

973 974 975 **References**

976
977 Ashpole, I., & Wiacek, A.: Impact of land-water sensitivity contrast on MOPITT retrievals and trends over
978 a coastal city, *Atmospheric Measurement Techniques*, 13(7), 3521–3542, [https://doi.org/10.5194/amt-13-](https://doi.org/10.5194/amt-13-3521-2020)
979 [3521-2020](https://doi.org/10.5194/amt-13-3521-2020), 2020.

980 Ashpole, I., and Wiacek, A.: Land- and water-only Level 3 products from MOPITT TIR-NIR Version 8 CO
981 retrievals, <https://doi.org/10.5683/SP3/ERCG2H>, Borealis, V1, 2022

982 Buchholz, R. R., Worden, H. M., Park, M., Francis, G., Deeter, M. N., Edwards, D. P., Emmons, L. K.,
983 Gaubert, B., Gille, J., Martínez-Alonso, S., Tang, M., Kumar, R., Drummond, J. R., Clerbaux, C., George,
984 M., Coheur, P-F., Hurtmans, D., Bowman, K. W., Luo, M., Payne, V. H., Worden, J. R., Chin, M., Levy,
985 R. C., Warner, J., Wei, Z., Kulawik, S. S.: Air pollution trends measured from Terra: CO and AOD over
986 industrial, fire-prone, and background regions, *Remote Sensing of Environment*, 256, 112275,
987 <https://doi.org/10.1016/j.rse.2020.112275>, 2021.

988 Buchholz, R. R., Park, M., Worden, H. M., Tang, W., Edwards, D. P., Gaubert, B., Deeter, M. N., Sullivan,
989 T., Ru, M., Chin, M., Levy, R. C., Zheng, B., Magzamen, S.: New seasonal pattern of pollution emerges
990 from changing North American wildfires, *Nature Communications* 13(2043),
991 <https://doi.org/10.1038/s41467-022-29623-8>, 2022

992 Deeter, M. N., Emmons, L. K., Francis, G. L., Edwards, D. P., Gille, J. C., Warner, J. X., Khattatov, B.,
993 Ziskin, D., Lamarque, J.-F., Ho, S.-P., Yudin, V., Attié, J.-L., Packman, D., Chen, J., Mao, D. Drummond,
994 J. R.: Operational carbon monoxide retrieval algorithm and selected results for the MOPITT instrument,
995 *Journal of Geophysical Research*, 108(D14), 4399, <https://doi.org/10.1029/2002JD003186>, 2003.

996 Deeter, M. N., Edwards, D. P., Gille, J. C., and Drummond, J. R.: Sensitivity of MOPITT observations to
997 carbon monoxide in the lower troposphere, *Journal of Geophysical Research Atmospheres*, 112(24), 1–9,
998 <https://doi.org/10.1029/2007JD008929>, 2007.

999 Deeter, M. N., Martínez-Alonso, S., Edwards, D. P., Emmons, L. K., Gille, J. C., Worden, H. M., Pittman, J.
1000 V., Daube, B. C. and Wofsy, S. C.: Validation of MOPITT Version 5 thermal-infrared, near-infrared, and
1001 multispectral carbon monoxide profile retrievals for 2000-2011, *Journal of Geophysical Research*
1002 *Atmospheres*, 118(12), 6710–6725, <https://doi.org/10.1002/jgrd.50272>, 2013.

- 1003 Deeter, M. N., Martínez-Alonso, S., Edwards, D. P., Emmons, L. K., Gille, J. C., Worden, H.M., Sweeney,
1004 C., Pittman, J. V., Daube, B. C., and Wofsy, S. C.: The MOPITT Version 6 product: Algorithm
1005 enhancements and validation, *Atmospheric Measurement Techniques*, 7(11), 3623–3632,
1006 <https://doi.org/10.5194/amt-7-3623-2014>, 2014.
- 1007 Deeter, M. N., Edwards, D. P., Gille, J. C., and Worden, H. M.: Information content of MOPITT CO profile
1008 retrievals: Temporal and geographical variability, *Journal of Geophysical Research: Atmospheres*,
1009 120(24), 12723–12738, <https://doi.org/10.1002/2015JD024024>, 2015.
- 1010 Deeter, M. N., Edwards, D. P., Francis, G. L., Gille, J. C., Mao, D., Martínez-Alonso, S., Worden, H.M,
1011 Ziskin, D., and Andreae, M. O.: Radiance-based retrieval bias mitigation for the MOPITT instrument:
1012 The version 8 product, *Atmospheric Measurement Techniques*, 12(8), 4561–4580,
1013 <https://doi.org/10.5194/amt-12-4561-2019>, 2019.
- 1014 Deeter, M., Francis, G., Gille, J., Mao, D., Martínez-Alonso, S., Worden, H., Ziskin, D., Drummond, J.,
1015 Commane, R., Diskin, G., and McKain, K.: The MOPITT Version 9 CO Product: Sampling Enhancements
1016 and Validation, *Atmos. Meas. Tech.*, <https://doi.org/10.5194/amt-2021-370>, <https://doi.org/10.5194/amt-15-2325-2022>, 2022.
- 1018 Drummond, J. R., Zou, J., Nichitiu, F., Kar, J., Deschambaut, R., and Hackett, J.: A review of 9-year
1019 performance and operation of the MOPITT instrument, *Advances in Space Research*, 45(6), 760–774,
1020 <https://doi.org/10.1016/j.asr.2009.11.019>, 2010.
- 1021 Drummond, J. R., Hackett, J., and Caldwell, D.: Measurements of pollution in the troposphere (MOPITT),
1022 in: *Optical Payloads for Space Missions*, edited by: Shen-En Qian, Wiley and Sons, West Sussex, UK,
1023 639–652, 2016.
- 1024 Duncan, B. N., Logan, J. A., Bey, I., Megretskaia, I. A., Yantosca, R. M., Novelli, P. C., Jones, N.B., and
1025 Rinsland, C. P.: Global budget of CO, 1988 - 1997: Source estimates and validation with a global model,
1026 *Journal of Geophysical Research Atmospheres*, 112(22), D22301, <https://doi.org/10.1029/2007JD008459>,
1027 2007.
- 1028 Edwards, D. P., Halvorson, C. M., and Gille, J. C.: Radiative transfer modeling for the EOS Terra satellite
1029 Measurement of Pollution in the Troposphere (MOPITT) instrument, *Journal of Geophysical Research*
1030 *Atmospheres*, <https://doi.org/10.1029/1999JD900167>, 1999.
- 1031 Francis, G. L., Deeter, M. N., Martínez-Alonso, S., Gille, J. C., Edwards, D. P., Mao, D., Worden, H. M.,
1032 and Ziskin, D.: Measurement of Pollution in the Troposphere Algorithm Theoretical Basis Document:
1033 Retrieval of Carbon Monoxide Profiles and Column Amounts from MOPITT Observed Radiances (Level
1034 1 to Level 2), *Atmospheric Chemistry Observations and Modelling Laboratory, National Center for*

1035 Atmospheric Research, Boulder, Colorado, downloaded from:
1036 https://www2.acom.ucar.edu/sites/default/files/mopitt/ATBD_5_June_2017.pdf, 2017.

1037 Hedelius, J. K., Toon, G. C., Buchholz, R. R., Iraci, L. T., Podolske, J. R., Roehl, C. M., Wennberg, P. O.,
1038 Worden, H. M., Wunch, D.: Regional and Urban Column CO Trends and Anomalies as Observed by
1039 MOPITT Over 16 Years, *Journal of Geophysical Research: Atmospheres*, 126(5), 1–18,
1040 <https://doi.org/10.1029/2020JD033967>, 2021.

1041 Lamarque, J. F., Emmons, L. K., Hess, P. G., Kinnison, D. E., Tilmes, S., Vitt, F., Heald, C. L., Holland, E.
1042 A., Lauritzen, P. H., Neu, J., Orlando, J. J., Rasch, P. J., and Tyndall, G. K.: CAM-chem: Description and
1043 evaluation of interactive atmospheric chemistry in the Community Earth System Model, *Geoscientific
1044 Model Development*, 5(2), 369–411, <https://doi.org/10.5194/gmd-5-369-2012>, 2012.

1045 MOPITT Algorithm Development Team: MOPITT (Measurements of Pollution in the Troposphere) Version
1046 8 Product User’s Guide, Atmospheric Chemistry Observations and Modeling Laboratory, National Center
1047 for Atmospheric Research, Boulder, downloaded from:
1048 https://www2.acom.ucar.edu/sites/default/files/mopitt/v8_users_guide_201812.pdf, 2018.

1049 NASA/LARC/SD/ASDC, 2000a. MOPITT Derived CO (Near and Thermal Infrared Radiances) V008.
1050 Available at: https://doi.org/10.5067/TERRA/MOPITT/MOP02J_L2.008.

1051 NASA/LARC/SD/ASDC, 2000. MOPITT CO gridded daily means (Near and Thermal Infrared Radiances)
1052 V008. Available at: https://doi.org/10.5067/TERRA/MOPITT/MOP03J_L3.008.

1053 Pan, L., Edwards, D. P., Gille, J. C., Smith, M. W., and Drummond, J. R.: Satellite remote sensing of
1054 tropospheric CO and CH₄: forward model studies of the MOPITT instrument, *Applied Optics*, 34(30),
1055 6976. <https://doi.org/10.1364/ao.34.006976>, 1995.

1056 Pan, L., Gille, J. C., Edwards, D. P., Bailey, P. L., and Rodgers, C. D.: Retrieval of tropospheric carbon
1057 monoxide for the MOPITT experiment, *Journal of Geophysical Research*, 103(D24), 32277.
1058 <https://doi.org/10.1029/98JD01828>, 1998.

1059 Rodgers, C. D.: *Inverse Methods for Atmospheric Sounding, Theory and Practice*, World Scientific,
1060 Singapore, 2000.

1061 Worden, H. M., Deeter, M. N., Edwards, D. P., Gille, J. C., Drummond, J. R., and Nédélec, P.: Observations
1062 of near-surface carbon monoxide from space using MOPITT multispectral retrievals, *Journal of
1063 Geophysical Research Atmospheres*, 115(18), 1–12, <https://doi.org/10.1029/2010JD014242>, 2010.

1064 Worden, H. M., Deeter, M. N., Edwards, D. P., Gille, J., Drummond, J., Emmons, L. K., Francis, G., and
1065 Martínez-Alonso, S.: 13 years of MOPITT operations: Lessons from MOPITT retrieval algorithm
1066 development, *Annals of Geophysics*, 56(FAST TRACK 1), 1–5, <https://doi.org/10.4401/ag-6330>, 2014.